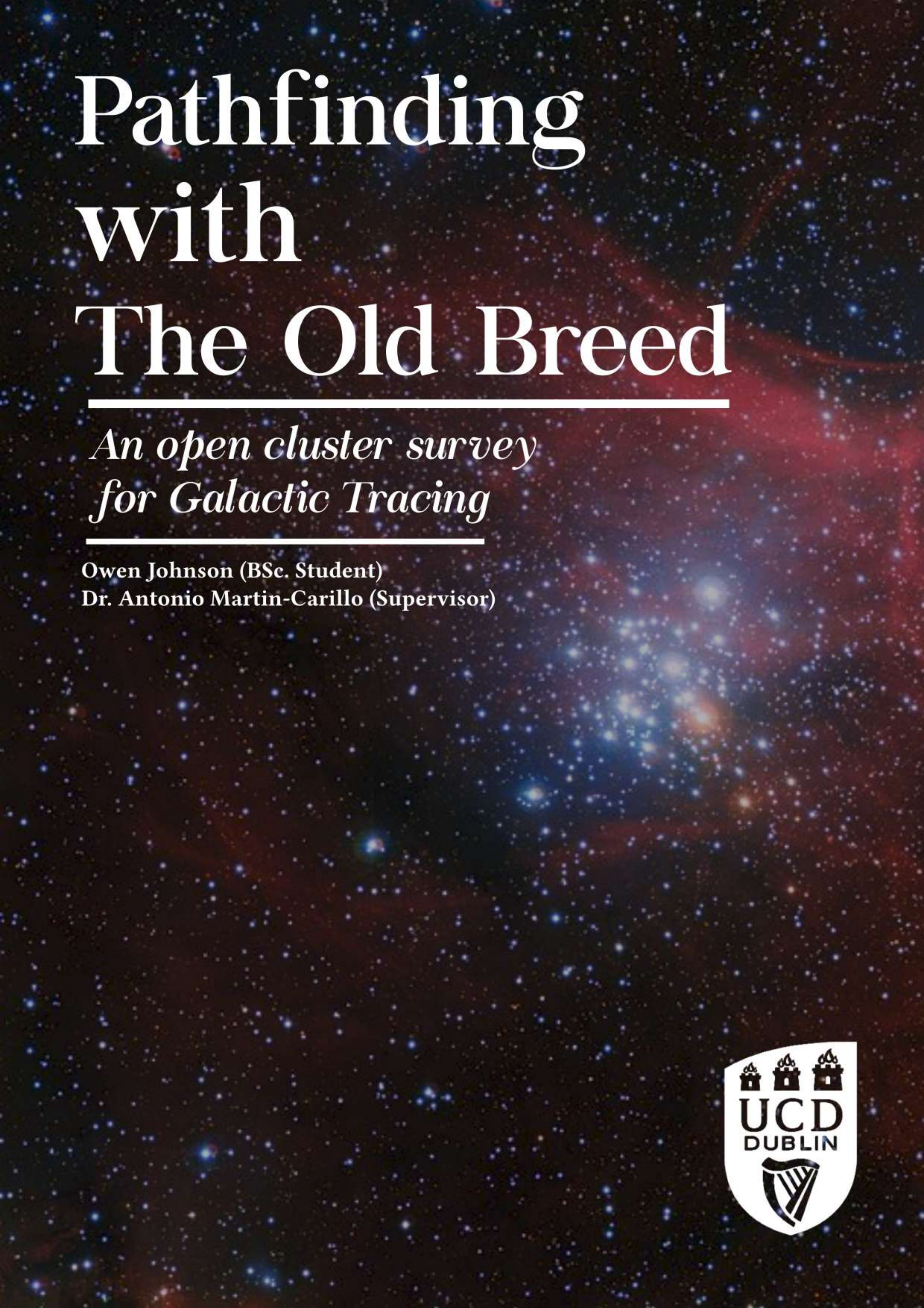

Pathfinding with The Old Breed

An open cluster survey for Galactic Tracing

Owen Johnson (BSc. Student)
Dr. Antonio Martin-Carillo (Supervisor)

Preface

This project was completed as part of a fulfilment of a BSc in Physics with Astronomy and Space Science (2018 - 22). It follows the form of a American Astronomical Society (AAS) style paper to teach the student the work-flow required to publish a scientific paper. This project did not follow the form of the conventional undergraduate thesis thus it is complied oddly into the following four documents.

1. Final paper: complete report of scientific findings from start to finish, formatted in AAS style.
2. Literature review: Review of previous material in the field used to plan the aims, objective and outcome of the project.
3. Data Analysis report: Summary of the analysis that was carried out on acquired data and how it fit into the proposal.
4. Observation Proposal: Proposal sent to Calar Alto Observatory detailing the justification for observation time and intended targets for the study.

Pathfinding with the Old Breed: Using the Old Clusters of the Milky Way for Galactic Tracing

Owen Johnson [1]

[1] School of Physics, University College Dublin, Ireland

ABSTRACT

Open clusters have been long used as stellar laboratories, and galactic tracers. In this study both are used in tandem to investigate the distribution of old (> 1000 Myr) open clusters in a milky way. BV photometric data were collected for Berkeley 28, Bochum 2, NGC 2124 and NGC 2155. Each cluster's population was determined using Gaia data and parameterised using MIST and DSEP isochrones, along with classification based on the Trumpler scheme and cataloguing of the stellar population. These clusters were combined with 266 open clusters from newly available catalogues to perform galactic tracing. It was found that there is an underabundance of old open clusters within the inner galactic disk of the Milky Way despite production outweighing disruptive dynamical forces in the galaxy. It is also shown that there is no direct correlation between cluster age and galactic position. This would indicate the sprawling embedment of older clusters throughout the milky way is due to a layered relationship between internal cluster dynamics and the disk environment. It is deemed that an underabundance of old clusters is due to dispersion as a result of destructive interactions and misrepresentation due to observational selection, with the old breed of open clusters found to be gradually inflating the galactic disk.

Keywords: Open Clusters & Associations — Galactic Tracing — Isochrone Fitting

This work is dedicated to my mentor and my friend Noel White, (1951-2021).

1. INTRODUCTION

Open clusters have been shown to be an integral part of the astronomer's toolbox, readily lending themselves as stellar laboratories. Open clusters are classified as a group of stars around the same age and loosely bound through mutual gravitation.
Their similar age allows for in-depth observation of the stellar evolution. Through this, many attributes of the stellar population can be inferred. As clusters span age ranges from a couple of Myr to Gyrs, many have been present since the formation of the disk itself. Through this, if clusters of varying ages are examined, it is possible to trace the evolution of the milky way.

Mapping the milky way has always been difficult, given the vantage point it can be observed from. This makes it quite challenging to appreciate the shape and dimensions of the milky way. Some of the pioneering studies, such as Herschel (1785); Shapley (1918) and Trumpler (1930) first outlined the use of open clusters to map the galaxy. Following with studies by Becker & Fenkart (1970) which pathed the spiral arms of the milky way using open clusters and numerous studies by van den Bergh (1958) which explore the evolution of the galaxies scale height.

More recent studies such as Bonatto et al. (2006) use young open clusters to predict shape evolution of the galaxy, by analysing longitudinal distribution of young clusters to predict reflected areas of star formation and presence of spiral arms. Other research using the homogeneity of open-clusters to analyse the chemical composition of the galaxy as they preserve abundances of gas from their formation, Dias et al. (2002) shows that chemical distribution is uniform with no intrinsic scattering making open clusters perfect for mapping the chemical evolution of the milkey way.

While the precision and accuracy of cluster age estimates are tied to the quality of the observational data and theoretical models, the process of estimating cluster age through the use of colour-magnitude diagrams is relativity straightforward and has been shown to be tried and true. Even early open cluster catalogues like Lyngå (1988) included distance estimates, while more recent catalogues like Koposov et al. (2008) have provided other parameters such as age, metallicity and excess colour. Furthermore, with the second data release from Gaia (GDR2; Gaia Collaboration et al. 2018) presenting the most in-depth all-sky astrometric and photometric study to date.

This increase in available data has allowed for the characterisation of open clusters on mass adding to catalogues such as WEBDA. Determination of all open clusters identified by Gaia is an ongoing task and is being automated using modern techniques and machine learning as shown in studies by Bossini et al. (2019) and Cantat-Gaudin et al. (2020).

This study used the 1.25 m optical telescope at the Calar Alto Observatory (CAHA) to observe four open clusters from the WEBDA catalogue. The aim of this work was to classify the four observed clusters and infer details of each cluster. After which the observational cluster parametrization was utilized in tandem with other larger studies to examine the distribution of old open clusters in the milky way investigating both the relation between the old clusters and galactic position. Exploring the effect the old breed have on the evolution of the milky way.

2. OBSERVATIONS

This study observed 4 open-clusters from the WEBDA database on the night of March 10th 2022. Each cluster was observed using B and V filters in the Johnson Cousins' *UBVI* system. The average observation time for each cluster was 210 s in each filter. Standard image calibration and reduction was carried out.

2.1. *Target Selection Strategy*

For this work it was important for the sample to observe clusters grouped at a similar area of the galactic disk (see. fig. 7) at varying estimated cluster ages, with each group containing an old (> 1000 Myr), young (< 100 Myr) and one intermediate cluster. In grouping the targets like this it would allow for comparison between galactic position and varied age, giving the most scientific value to the small quantity of clusters analysed.
The observed targets are listed in table 1. A further six open clusters from the WEBDA catalog are also analysed to add to the sample size of clusters analysed and classified by the methods of this work. The six cluster initially proposed for observation were not observed due to poor conditions during the observation period.

2.2. *Photometry*

Photometric analysis was carried out by first using `DAOStarFinder` with an FWHM chosen as the average of moderate sources to favour an array of sources. Aperture photometry is performed as standard. To try to maximize the accuracy of magnitudes from each source, trial apertures were tested on each source. The aperture which corresponded to the highest SNR value was identified. The aperture for each max SNR value was noted, with the final used aperture value used taken to be the mean value of all sources apertures that did not exceed an SNR value of 50 or greater. Much like the choice around the FWHM value, this choice was used to optimize the accuracy of the magnitudes attained.

2.2.1. *Magnitude Calibration*

The instrumental magnitude was calibrated to real magnitude using the 9th data release of the AAVSO Photometric All-Sky Survey (APASS9). Each source was queried to the APASS9 catalogue. If a source in the catalogue was within 3 pixels (1.806 arsecs) of the source centroid position, the query was considered a match and respective real (M_{real}) and instrumental magnitudes ($M_{\text{inst.}}$) were saved.
A linear relationship was formed between M_{real} and $M_{\text{inst.}}$ and used for instrumental conversion. The error on both the slope (σ_m) and constant (σ_c) was taken as the square roots of each ones respective diagonal entries in the outputted covariance matrix.

2.2.2. *Error on Magnitude*

As this study also catalogues 4 clusters, it was important to quantify error on each collected magnitude. For this §6 of Bevington & Robinson (2003) was followed closely. This allowed for errors on $M_{\text{inst.}}$ to be ascribed to M_{real} using the derivative and added to quadrature in $M_{\text{inst.}}$. Then using the full covariance matrix for propagation through a fitted function gave an error for converted magnitudes, taking both the APASS's systematic error and the instrumental error given by SNR ($\Delta M \sim 1/\text{SNR}$) and combining.

$$\sigma_{M_{conv.}} = \sqrt{M_{\text{inst.}}^2 \sigma_m^2 + \sigma_c^2 + 2M_{\text{inst.}}\sigma_{mc}^2} \qquad (1)$$

Where $M_{conv.}$ is the converted magnitude and m and c are the slope and constant of the linear fit. The covariance cross-term σ_{mc} was considered negligible due to the internal precision of `numpy.float`.

3. POPULATION DETERMINATION

After their identification, the main obstacle in studying open clusters is determining the validity of a source's membership in the population. This problem can often

Table 1. List of analysed targets.

Target Cluster	RA (J2000)	DEC (J2000)	WEBDA Study
	hh:mm:ss	deg:mm:ss	
Berkeley 28	06:52:12	02:56:00	Mohan et al. (1988)
Bochum 2	06:48:54	00:23:00	Turbide & Moffat (1993)
NGC2324	07:04:07	01:02:42	Kyeong et al. (2001)
NGC2355	07:16:59	13:45:00	Kaluzny & Mazur (1991)
Proposed Open Clusters			
Berkeley 20	05:33:00	00:13:00	Durgapal et al. (2001)
Berkeley 34	07:00:24	-00:15:00	Ortolani et al. (2005)
King 1	00:22:04	64:22:50	Lata et al. (2004)
King 15	00:32:54	61:52:00	Phelps & Janes (1994)
NGC 2129	06:00:41	23:19:06	Carraro et al. (2006)
Stock 18	00:01:37	64:37:30	Bhatt et al. (2012)

NOTE—Above details the targets analysed throughout this work. The first four targets were obsereved at CAHA. With the following six grouped as the proposed clusters. The associated WEBDA study used for supplementation is also listed.

be negated by using spatial distribution to determine which stars pose likely candidates. This method has seen some success as seen in studies by Schilbach et al. (2006) and also in the study of globular clusters as recently shown by Valle et al. (2022). This method however, falls short when dealing with clusters that have a moderate to low degree of concentration and no discernable shape as with the majority of open clusters.

The field of determining cluster populations is one that sees frequent studies, but there is no one particular method widely accepted. One promising study is Stott (2018) which approaches the problem on the basis of photometric membership using Bayesian statistics, which would remove the reliance on supplementary astrometric or spectroscopic data.

However, this study incorporates the use of Gaia's second data release values on stellar parallax as a means to determine cluster population as the former method currently requires open-clusters to have photmetric data in the U filter.

3.1. *Using Gaia*

This study takes full advantage of Gaia's DR2. Each observed cluster is queried, collecting entries for stars within 10 arcmins of the cluster centre. Each returned entry then was filtered based on the associated error on the G-band mean magnitude with values of < 0.01 accepted.

A hierarchical density-based scan (HDBSCAN) was then used on the parallactic data to determine possible members of the population.

A density-based scan or DBSCAN is an algorithm first coined by Ester et al. (1996). DBSCAN works given two parameters a linking length, ϵ and minimum neighbourhood point. An illustration of this can be seen in fig. 1, where a point is considered a neighbour if it falls within the linking distance of another point and is then considered a set once the defined threshold for cluster size is met.

A HDBSCAN is a descendant of DBSCAN created by Campello et al. (2013). In the case of HDBSCAN, there is no dependency on linking (ϵ) and instead, pruning nodes that do not meet the star population threshold and re-analysing the ones that do. The minimum clustering value for each cluster was taken as 3 times the number of parallax values that had been standardized by centering and scaling using `sklearn.StandardScaler`.

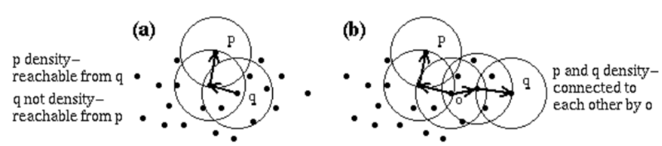

Figure 1. Example of DBSCAN selection showing how points are linked together. Figure courtesy of Ester et al. (1996).

The benefits of using parallax compared to photometric data can be seen in fig. 2. Where usually DBSCAN or HDBSCAN would remove stars that are off the main sequence, the parallax retains the non-main-sequence population. As this scan performs on a hierarchical basis,

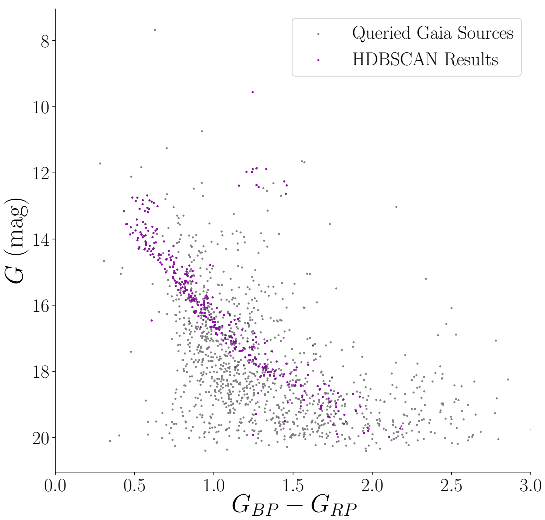

Figure 2. Stellar population determined for NGC 2355 using Gaia parallax data and HDBSCAN method.

the probability of a star being part of a cluster is related to the 'distance' between the first ('birth') cluster and the last cluster ('death'). The persistence of a cluster is expressed as $\lambda = \frac{1}{\text{distance}}$, where distance is the distance from the core cluster. The persistence of birth and death is then λ_{birth} and λ_{death} respectively.
The stability of a classified cluster is then

$$\text{stablity} = \sum_{p \in \text{cluster}} (\lambda_p - \lambda_{\text{birth}}) \quad (2)$$

The probability of a star in a cluster is then classified as the normalised corresponding stability. The results of this classification can be found in table 2. The uncertainty on the population is taken as the proportion of the population that had 80% or less membership of probability. The expected population in table 2 is taken from Cantat-Gaudin et al. (2020), and in the case of Bochum 2, taken from Turbide & Moffat (1993).

Table 2. Results of Gaia population classification.

Target	Population	Study Population
Berkeley 28	79 ± 17	53
Bochum 2	110 ± 13	110
NCG 2324	251 ± 26	242
NGC 2355	139 ± 128	261

Determining the population through the use of HDBSCANs and Gaia provided promising results. Each cluster responded to the filtering with the underestimations seen in NGC 2123 in part due to stars with a magnitude of 19 or greater. However, the calculated probabilities had varying results in quantifying the uncertainty of cluster population. For the more sparsely populated clusters such as Berkeley 28, Bochum 2 and NGC 2324, the probabilities returned a mean membership rate of 89%, 92%, and 95%, respectively. While these estimations appear adequate and are in line with the ranges shown for these clusters in similar studies (Bossini et al. 2019; Mohan et al. 1988; Frandsen & Arentoft 1998; Kaluzny & Mazur 1991) the population of each cluster should be around a 30% underestimation given the distribution of brightness in each cluster.

4. DETERMINING CLUSTER PARAMETERS

Following the cluster population analysis the next step is fitting parameters to the set of observed and proposed open-clusters.

4.1. *Isochrones*

4.1.1. *Detailing MIST and DSEP*

The isochrones generated for use in this study were created using the MESA Isochrones and Stellar tracks (MIST; Choi et al. 2016) from the Modules for Experiments in Stellar Astrophysics (MESA; Paxton et al. 2018). MIST uses the Sun as a basis for its chemical compositions, with solar abundances modelled by Asplund et al. (2009) with $Z_\odot = 0.014$. MIST takes hot wind-driven mass-loss from Vink et al. (2001), cooled dust driven mass loss from de Jager et al. (1988) and Nugis & Lamers (2000) for any mass loss in the helium star phase. With convection boundaries modelled after Ledoux (1947) and convection overshooting modelled using Herwig (2000).
The Dartmouth Stellar Evolution Database (DSEP) was also used to supplement fitting where MIST mass limits became constrictive at later ages. The DSEP isochrones are based on models outlined by Dotter et al. (2008).

4.1.2. *Using MIST and DSEP*

The choice of using MIST was due to its recent creation compared to WEBDA used isochrones (Padova & Geneva) and also it's ease of interpolation compared to other commonly used ioschrones such as PARSEC. A detailed comparative study of popular modern isochrones is carried out by Agrawal et al. (2022).
Interpolation and plotting was carried out using a forked version of the `isochrones` package created by Morton (2015). `isochrones` possessed a high functioning front end for accessing MIST isochrones from the Johnson UBVI system and plotting with minimal turnaround time. This allowed for quick incremental change in the

parameters generating isochrones making the process for incrementally fitting isochrones less cumbersome.

4.2. *Isochrone Results*

Isochrone fitting was carried out on 10 clusters as listed in table 1. The 4 observed clusters, Berkeley 28, Bochum 2, NGC 2324 and NGC 2355, along with the 6 proposed clusters. The resultant parameters from these fits can be seen in table 3.
Each cluster's parameters were compared to both their corresponding WEBDA study and Cantat-Gaudin et al. (2020) to compare values. Of the 4 observed clusters, the 2 youngest clusters Bochum 2 (Bo 2) and Berkeley 28 (Be 28) did not show any discernable main sequence. This can be clearly seen in fig. 4 (a, b). This is due to their smaller population size compared to the older NGC clusters. In the case of Be 28, when fitting, the age was assumed from Mohan et al. (1988) and then interpolated to best fit observed data. Similarly Bo 2 could have had a many potential fits, also not having a main discernable sequence. Here the shape of CMD produced by Turbide & Moffat (1993) was consulted to ensure a somewhat meaningful fit. A further observation using further UVB data or photometric Gaia would provide a more credible parameterisation. Of the proposed clusters, all parameters fell within the agreement of WEBDA associated studies (table 1), Bossini et al. (2019) or Cantat-Gaudin et al. (2020).

4.3. *Goodness of Fit*

Fitting isochrones in itself can be an unwieldy task and often difficult to quantify the 'goodness' of fit. In this case, the isochrone was first fitted by varying values of colour to find the extinction in the V band using the following expression as per (Dyson & Williams 1980, pg. 237).

$$A_v = 3.1\ E(B-V) \quad (3)$$

The distance was then determined by taking into account the value for extinction. Both age and metallicity were determined by fitting various incremental parameters by eye and taking the 'best' fit as the value of the parameter. The errors were taken to be the limits where the parameters argued for being a 'good' fit. While not a quantitative or rigorous method for justifying a data fit, it has historically provided results with an adequate degree of confidence. The release of GDR2 has prompted a new wave of studies developing means of attaining tangible goodness of fit for modern isochrones. Valle et al. (2021) has coined a promising method of Mahalanobis distances of stellar data points to plotted isochrones and mask resultant synthetic CMDs with χ^2 distributions to fit Gaia samples as a means of seeing if a fit is good.

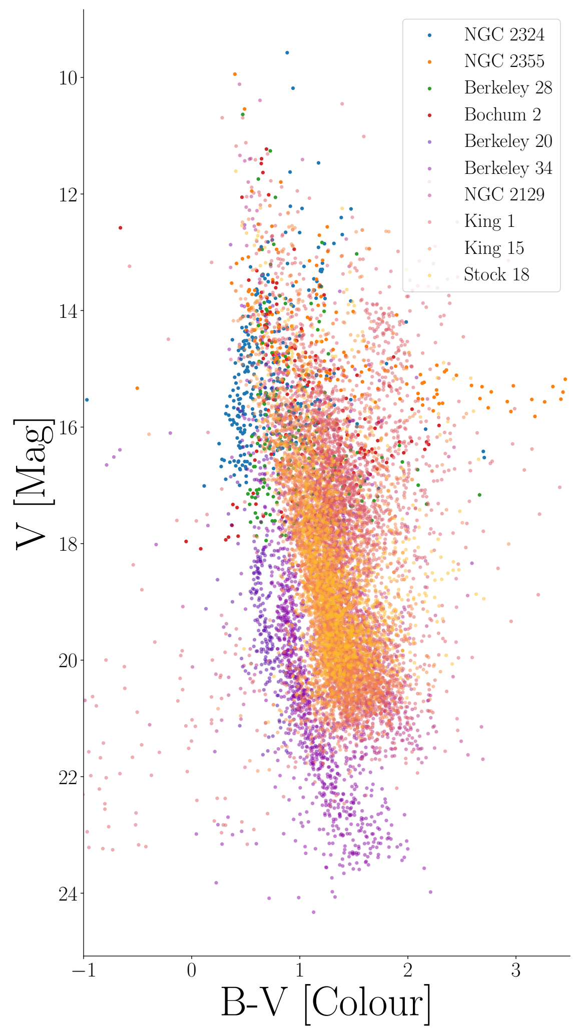

Figure 3. Overall CMD plot of all stars analysed in this study. This illustrates homogenity of the stellar population distributed along the main-sequence. Each colour representing an open cluster.

5. CLASSIFICATION

5.1. *Open Cluster Classification Scheme*

Open clusters span many different distributions in density, size, and stellar constituents. Open clusters can

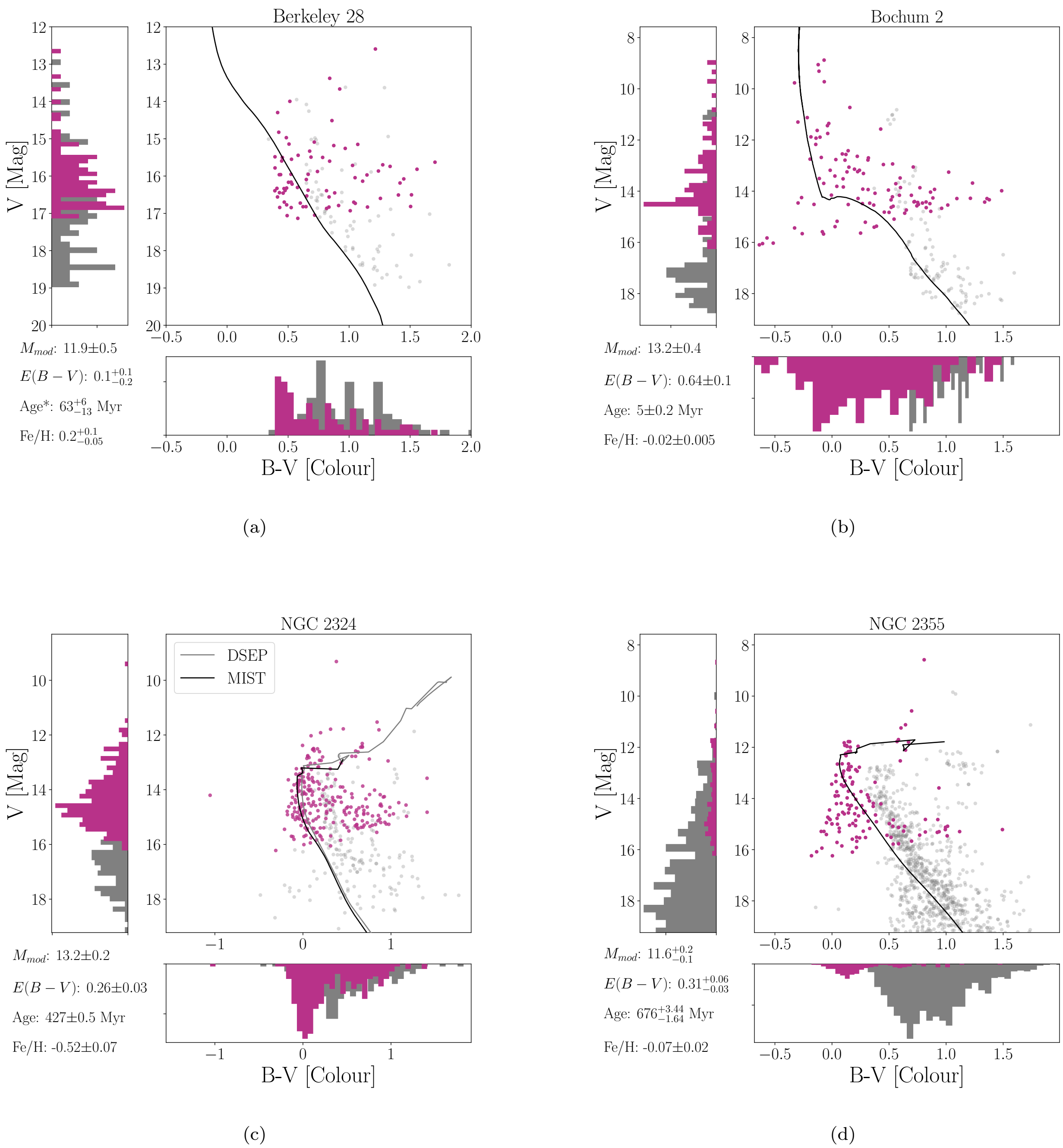

Figure 4. Colour magnitude diagrams fitted to MIST isochrones of observational data with complementary WEBDA data plotted in grey. Histogram on each the x and y axis represent distribution of colour and magnitude respectively.

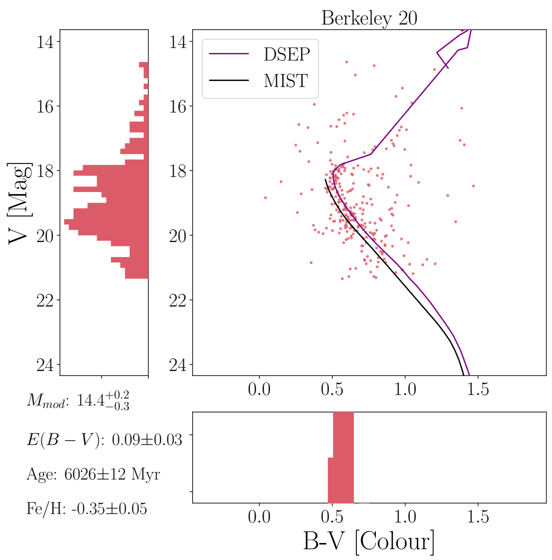

Berkeley 20
DSEP
MIST
V [Mag]
B-V [Colour]
M_{mod}: $14.4^{+0.2}_{-0.3}$
$E(B-V)$: 0.09±0.03
Age: 6026±12 Myr
Fe/H: -0.35±0.05

(a)

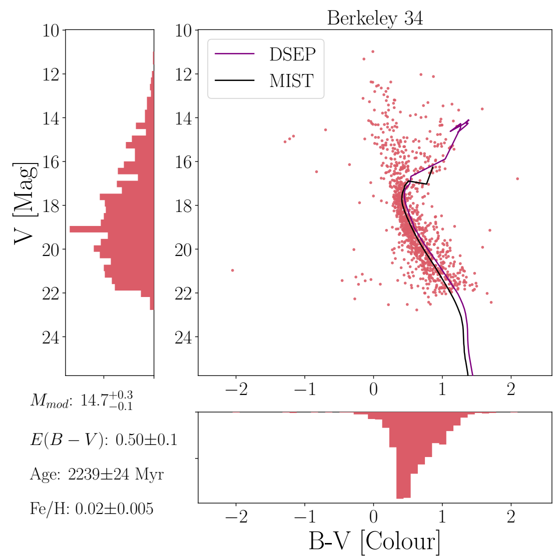

Berkeley 34
DSEP
MIST
V [Mag]
B-V [Colour]
M_{mod}: $14.7^{+0.3}_{-0.1}$
$E(B-V)$: 0.50±0.1
Age: 2239±24 Myr
Fe/H: 0.02±0.005

(b)

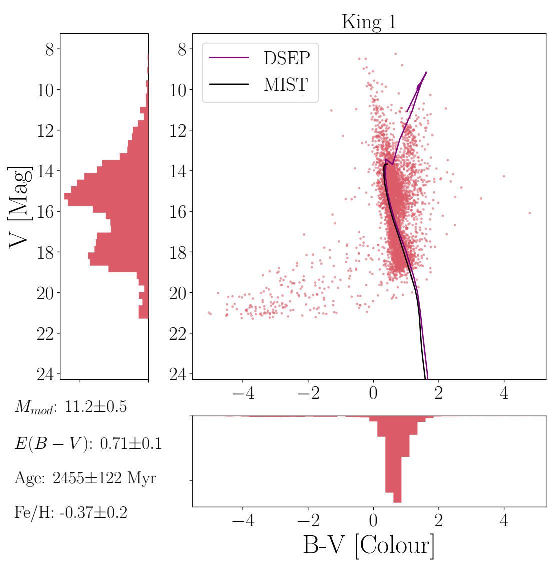

King 1
DSEP
MIST
V [Mag]
B-V [Colour]
M_{mod}: 11.2±0.5
$E(B-V)$: 0.71±0.1
Age: 2455±122 Myr
Fe/H: -0.37±0.2

(c)

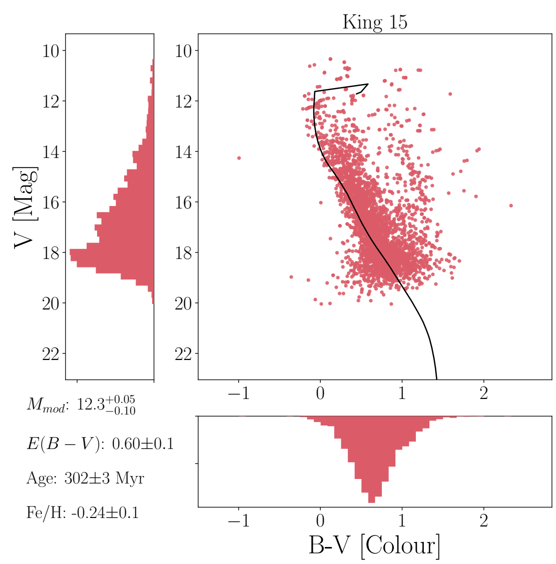

King 15
V [Mag]
B-V [Colour]
M_{mod}: $12.3^{+0.05}_{-0.10}$
$E(B-V)$: 0.60±0.1
Age: 302±3 Myr
Fe/H: -0.24±0.1

(d)

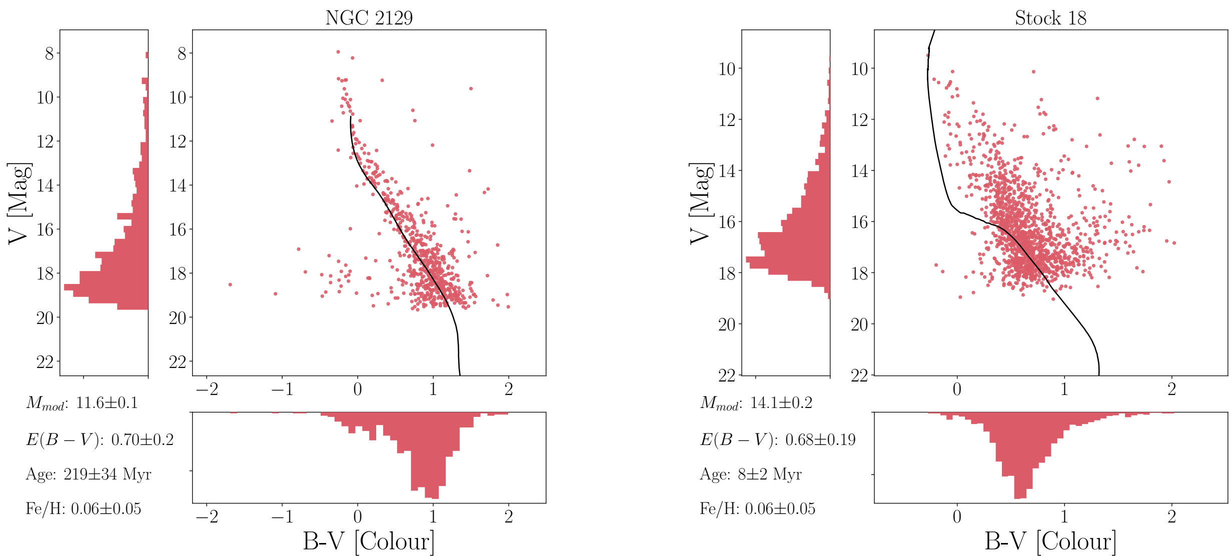

(e) (f)

Figure 5. Colour magnitude diagrams fitted to MIST isochrones of observational data with complementary WEBDA data plotted in grey. Histogram on each the x and y axis represent distribution of colour and magnitude respectively.

Table 3. Cluster parameters.

Cluster	Age		Distance		Colour		Metalicity		Extinction	
	Myr		M_{V_0}		$E(B-V)$		Fe/H		A_v	
	Obs.	*Study*	*Obs.*	*Study*	*Obs.*	*Study*	*Obs.*	*Study*	*Obs.*	*Study*
Berkeley 28	63^{+6}_{-13}	$70\pm\cdots$	$11.9^{+0.5}_{-0.5}$	$12.2\pm\cdots$	$0.1^{+0.05}_{-0.05}$	$0.8\pm\cdots$	$0.2^{+0.1}_{-0.05}$	$\cdots$	0.31 ± 0.16	$2.48\pm\cdots$
Bochum 2	$5^{+0.2}_{-0.2}$	$\cdots$	$13.2^{+0.4}_{-0.4}$	$13.6\pm\cdots$	$0.64^{+0.1}_{-0.1}$	$0.31\pm\cdots$	$-0.02^{+0.005}_{-0.005}$	$\cdots$	1.98 ± 0.31	$0.85\pm\cdots$
NGC 2324	$427^{+0.5}_{-0.5}$	708 ± 36	$13.2^{+0.2}_{-0.2}$	$13.1\pm\cdots$	$0.26^{+0.03}_{-0.03}$	0.17 ± 0.12	$-0.52^{+0.07}_{-0.07}$	-0.32	0.81 ± 0.09	0.53 ± 0.06
NGC 2355	$676^{+3.44}_{-1.64}$	$708\pm\cdots$	$11.6^{+0.2}_{-0.2}$	12.1 ± 0.3	$0.31^{+0.06}_{-0.03}$	$0.12\pm\cdots$	$-0.07^{+0.02}_{-0.02}$	0.13	0.96 ± 0.12	$0.37\pm\cdots$
Berkeley 20	6026^{+12}_{-12}	$5000\pm\cdots$	$14.4^{+0.2}_{-0.3}$	15.1 ± 0.8	$0.09^{+0.03}_{-0.03}$	$0.13\pm\cdots$	$-0.35^{+0.05}_{-0.05}$	-0.75	0.28 ± 0.09	$0.40\pm\cdots$
Berkeley 34	2239^{+24}_{-24}	2300 ± 400	$14.7^{+0.3}_{-0.1}$	15.4 ± 0.1	$0.5^{+0.1}_{-0.1}$	0.3 ± 0.05	$0.02^{+0.005}_{-0.005}$	$\cdots$	1.55 ± 1.33	0.16 ± 0.05
King 1	2455^{+52}_{-52}	1585 ± 198	$11.2^{+0.5}_{-0.5}$	$13.6\pm\cdots$	$0.7^{+0.1}_{-0.1}$	0.7 ± 0.05	$-0.37^{+0.2}_{-0.2}$	$\cdots$	2.21 ± 0.22	2.17 ± 0.11
King 15	302^{+30}_{-30}	$3000\pm\cdots$	$12.3^{+0.05}_{-0.10}$	$13.4\pm\cdots$	$0.6^{+0.1}_{-0.1}$	$0.46\pm\cdots$	$-0.24^{+0.1}_{-0.1}$	$\cdots$	1.85 ± 0.19	$1.42\pm\cdots$
NGC 2129	219^{+34}_{-34}	$10\pm\cdots$	$11.6^{+0.1}_{-0.1}$	11.7 ± 0.3	$0.7^{+0.1}_{-0.2}$	0.8 ± 0.08	$0.06^{+0.05}_{-0.05}$	$\cdots$	2.10 ± 0.40	2.48 ± 0.20
Stock 18	8^{+2}_{-2}	6 ± 2	$14.1^{+0.2}_{-0.2}$	14.4 ± 1.02	$0.7^{+0.2}_{-0.2}$	0.8 ± 0.10	$0.06^{+0.05}_{-0.05}$	$\cdots$	2.10 ± 0.40	2.48 ± 0.31

Note—The above table contains the determined value for both observed and proposed clusters along with the relevant WEBDA collected data by authors outline in table 1. Values marked with (...) indicated where a respective study did not state the associated value. *Obs.* columns indicate parameters inferred from this work where *study* detail the parameters from associated studies. Errors on age is taken as a percentage error from inputted log age. Likewise errors on extinction are taken as a percentage error from colour excess.

contain large stellar agglomerations to just a handful of stars. While classification systems can vary based on the context of the study, the scheme coined by Trumpler (1930) sees prominent use.
This scheme classifies clusters based on three factors of the stellar population. a) their range of brightness, b) degree of concentration, and c) star population in the cluster. The details of this classification scheme can be seen in table 4. In this study, each observed target is classified based on this scheme.

5.2. *Classification Results*

Category a) of each cluster was classified based on the distribution of V magnitude which can be seen on the y-axis of fig. 5 along with the consideration of the average difference between V_{A_v} magnitudes of the confirmed stellar population, denoted $\Delta\bar{V}_{A_v}$. Category b) was determined using the concentration of each cluster based on distribution of confirmed stars from the cluster's center and visual appearance of the cluster as seen in appendix A. The final category c) was determined using the results of table 2.
The results of each classification can be seen in table 5. Each cluster was deemed to match Lynga (1981) or classification presented in associated WEBDA study (table 1).

5.3. *Cataloging*

Stars that were confirmed as part of the population have been cataloged with their respective parameters and can be found in appendix B. Each uncertainty takes into consideration the method described in section 2.2, along with the propagation of uncertainty given to both color excess and extinction as given in table 3.

6. SUPPLEMENTARY DATA FOR TRACING

This study directly uses 260 clusters catalogued by Cantat-Gaudin et al. (2020) to aid the observational sample size. This study also uses 269 clusters catalogued by Bossini et al. (2019) in use as a comparison to determining observational parameters. When searching for studies to complement this work, use of Gaia's second data release (DR2) was given preference. The reason for the use of supplementary data was to provide a more varying survey of the galactic disk. The first data set implemented was 269 clusters analysed and catalogued by Bossini et al. (2019). Their data set contains a large sample of clusters analysed from Gaia DR2, with each of the clusters containing a high degree of homogeneity among the stellar population. The cluster populations were determined using Bayesian methods of statistics along with DR2 astrometric data. In doing this, the probability of each star being a member of each cluster was 70% or greater. The parameters of each cluster were found using PARSEC isochrones (Bressan et al. 2012). This data set worked well to fill out a sample size in the galactic disk, as seen in fig. 7. Although this survey contained a good amount of clusters of varying ages, it lacked a significant number of older clusters of the milky way. To address this gap, 260 old clusters from Cantat-Gaudin et al. (2020) were used. This study used a neural network trained on high accuracy data sets to estimate cluster parameters using GDR2 parallax values and photometry ($G \leq 18$).

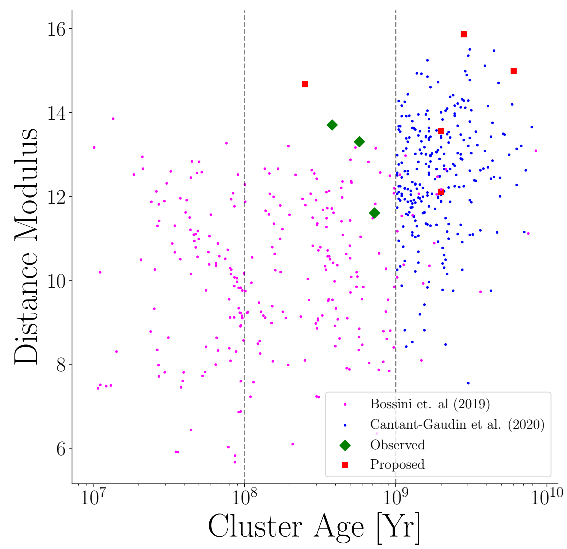

Figure 6. Distance against the log age of both observed targets, proposed targets and supplementary targets. This plot illustrates the gap of old clusters from Cantat-Gaudin et al. (2020)'s data fills.

7. GALACTIC TRACING

Following the classification of the four observed clusters and parameterising of the 10 clusters (proposed & observed), their age and location were used to make an enquiry into the present shape of the galactic disk. Here Cantat-Gaudin et al. (2020) sample of old open clusters is used fully. A preliminary caveat is the use of the term 'inner-disk'. For this work, as with similar studies, the inner disk is taken to be clusters that fall within a galac-

Table 4. Trumpler classification scheme.

Range of Brightness (a)	Degree of Concerntration (b)	Cluster Population (c)
1 - Majority of stellar objects show similar brightness.	I - Strong central concentration (Detached) (Detached)	p - Poor ($n < 50$)
2 - Moderate brightness ranges between stellar objects.	II - Little central concentration (Detached)	m - Medium ($50 < n < 100$)
3 - Both bright and feint stellar objects	III - No disenable concentration	r - Rich ($n > 100$)
	IV - Clusters not well detached (Strong field concentration)	

Note—Where n denotes the amounts the stellar population in a given cluster. For example Pleiades is a I3rn cluster and Hyades is a II3m cluster. Where the 'n' flag on a classification relates if the cluster shows nebulosity.

Table 5. Results of Trumpler classification on observed targets.

Target	ΔV_{mag}	ΔB_{mag}	σ_c	Population	Classification
Berkeley 28	1.73 ± 0.18	10.02 ± 0.50	2.989	79 ± 17	I1m
Bochum 2	10.60 ± 0.30	2.11 ± 0.20	3.263	110 ± 13	I3r
NGC2324	5.76 ± 0.20	4.90 ± 0.12	2.733	251 ± 26	II2r
NGC2355	2.20 ± 0.19	6.72 ± 0.14	2.517	139 ± 128	II2r

Note—Where n denotes the amounts the stellar population in a given cluster. For example Pleiades is a I3rn cluster and Hyades is a II3m cluster. Where the 'n' flag on a classification relates if the cluster shows nebulosity.

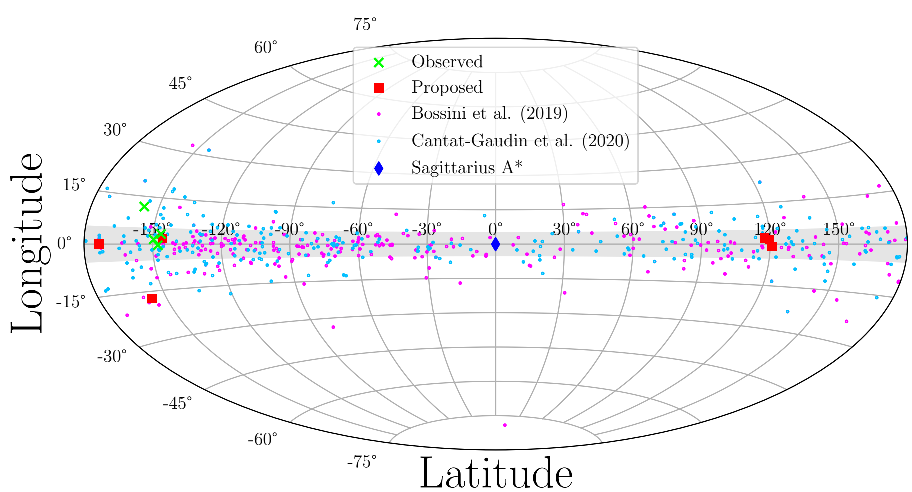

Figure 7. Aitoff projection of targets in terms of galactic co-ordinates, longitude (l) and latitude (b). Targets observed at CAHA are show by × (lime), the original proposal targets shown in boxes (red) and studies by Bossini et al. (2019) (pink) and Cantat-Gaudin et al. (2020) (sky blue). With the shaded region an approximate representing the galactic disk from $-5°$ to $+5°$

tocentric distance smaller than the Sun. This value[1] is taken to be 8180 ± 35 pc given by Gravity Collaboration et al. (2019).

7.1. *Distribution of Old Clusters*

The sample size collected for this study includes old open clusters from across the galactic disk at varying distances, as seen in fig. 7 and fig. 6. Plotting the distribution of these clusters can be seen in fig. 8.
The immediate takeaway from this depiction is the lack of older open clusters within the inner disk. Out of the 265 old clusters present, only 62 (23.8%) reside within the inner galactic disk. Moreover, looking at the distribution of ages as a function of both galactocentric radii.

7.2. *Reasons for Underabundance*

Trying to determine a reason for the underabundance seen in an older open cluster in the inner galactic disk has been a question since the start of using open clusters in galactic tracing. Oort (1950) assumed uniform star formation in the disk and initially deemed it to be a case of extrapolation of younger clusters as open clusters, which were much less prominent by nature.
The most intuitive explanation would be that over time both gravitational pull and destructive tidal forces would cause any open cluster to be pulled apart and dissipate into other surrounding objects, such as more massive clusters, through long term interactions.
Kaliberda (1973) derives a model for the evaporation of stars from open clusters based on the mass distribution of open clusters and applies the model to the Pleiades, predicting that all open clusters are dissipating. More recently, Angelo et al. (2019) confirmed the decline in stellar population in 6 open clusters. This distribution is based on dynamic simulations of age, limiting radius, stellar mass, and velocity dispersion. Looking outside the realms of internal dynamics in the cluster causing dispersion, there are also interactions with other objects in the galactic disk, causing cluster degeneracy acceleration. The primary suspect in these disruptive interactions is a massive dust cloud in the galactic core, as first noted by Spitzer (1958). Here it was stated that for a cluster of a mean density of $M_{\odot}/\mathrm{pc}^3$ the dispersion time would be ~ 200 Myr. Such that lower mass clusters would disperse at a much faster rate.
While the preceding arguments have both logic and evidential basis for these findings, open clusters increasingly disperse with time. There are a few points of interest to be raised that would contradict.

7.3. *Relating Cluster Age to Galactic Position*

The interesting consideration is that despite the internal and external interactions discussed in the previous section, there is still an appreciable amount of older clusters close to the galactic disk. Berkeley 17 (10 Gyr) and Collinder 261 (8 Gyr) are both within 200 pc of the plane. As Cantat-Gaudin et al. (2020) discusses since the release of GDR2 confirmation of 9 old clusters[2] within $R_{GC} < 6500$ pc. Small parallax coupled with sparse CMDs, as illustrated by Be 28 indicates that there could be more clusters located deeper in the disk within this region. However, difficulty inferring their parameters prevents meaningful estimates of distance.
The first large scale catalogues of open clusters by Lynga (1982) and Dias et al. (2002) suggest that destructive forces are too efficient to relate to the amount of older clusters currently seen.

Figure 9 shows no clear relationship between the age of a given cluster and its galactocentric radius. As shown by fig. 8 most of the old clusters lie outside the inner disk, with 4 of the clusters under 1000 Myr also situated outside the inner disk. When looking at fig. 10, there is also no clear relationship between age and cluster present in the bulge. The extreme outliers of clusters like Be 20 could be residual formation from an interaction of more populous clusters near the bulge.
Given these factors, it is likely that the relationship between cluster age and position in the galactic plane is a nuanced relationship between inherent cluster properties, internal dynamics and the overall environment in the galaxy.
An extension to this study would be to use GDR2 to investigate the orbits of old and ancient open clusters. It has been shown in a study by **?** that older open clusters adhere to extensive elliptical orbits. If these orbits were simulated on a large enough time scale it could show a migration pattern into the inner disk. It would also be worthwhile to further explore the internal dynamics of the cluster, finding a relation between the initial mass of older open clusters and the strength of their gravitational bounds. Another reason less open clusters are seen point to the inner disk. There also could be observational selection at play, as previously stated, with asterism and difficulty differentiating older clusters from concentrated areas in the disk. These findings are also echoed in Bonatto et al. (2006).

7.4. *Galatic Evolution*

[1] Currently the most accurate accepted value for solar distance to Sagittarius A*

[2] NGC 6005, NGC 6583, UBC 307, UBC 310, UBC 339, LP 866, UFMG 2, Ruprecht 134, and Teutsch 84

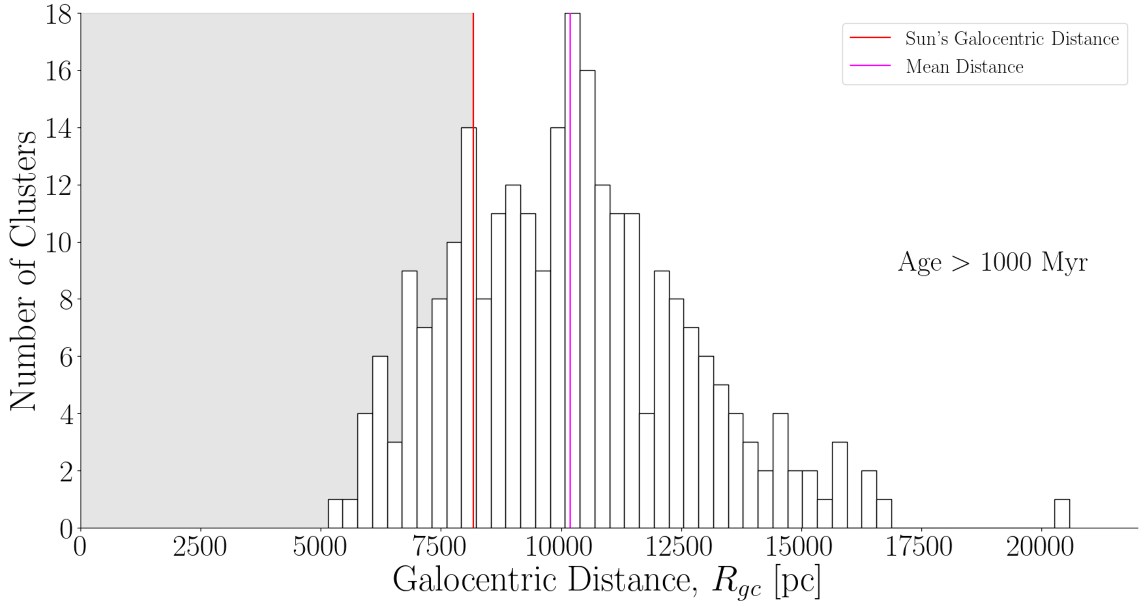

Figure 8. Distribution of old clusters according to galocentric distance. This sample includes 10 clusters of this work and 260 old open clusters from Cantat-Gaudin et al. (2020). The inner disk region is shaded.

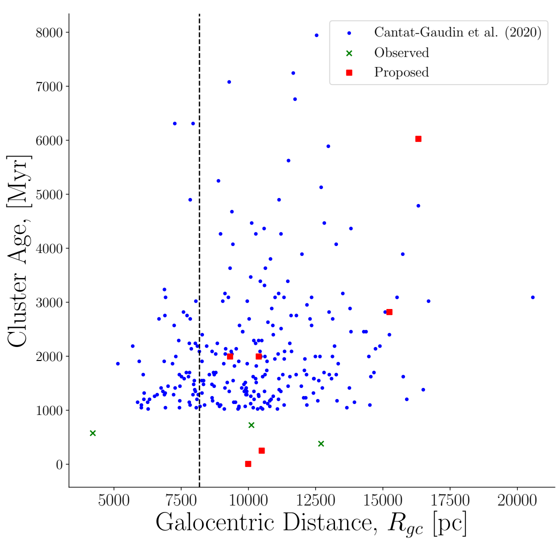

Figure 9. Plot of cluster age against distance galocentric distance, $R_{\rm gc}$. Errors were too small to be adequately displayed, see table 3 for specific values.

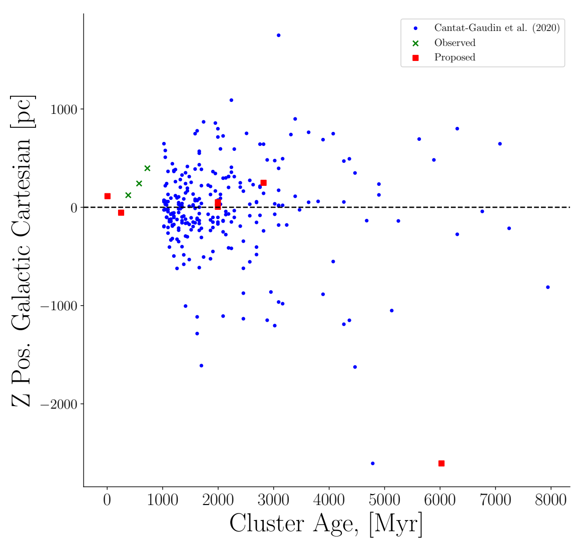

Figure 10. Plot of cluster age against galactic cartesian coordinates in the z-direction, Z.

Regardless of the reasons for potential underabundances in the inner galactic disk, most old clusters are in the outer disk. The excursion of old open clusters to more considerable galactocentric distances away from disruptive interactions appears highly asymmetric. This also shows that old open clusters are contributing to thickening of the galactic disk. The old open clusters indicate that there is a higher displacement of clusters in the Z direction[3] at higher values of galactocentric distances. This means that as young clusters migrate from

[3] Z values for clusters were taken from respective WEBDA studies.

the spiral arms by disruptive forces, the outer regions of the disk will become inflated compared to the bulge. This prediction follows two assumptions; a) the production of open clusters outweighs the disruptive dynamics of the galaxy as shown by Janes et al. (1988), and b) that the rate of dissipation of old clusters remains stable in outer regions where, by nature, there are fewer disruptive interactions compared to the inner disk.

8. CONCLUSIONS

This study collects BV data on four clusters from the WEBDA catalogue. Each observed cluster was classified based on Gaia's second data release exclusively through hierarchical density-based scanning. Each cluster was characterised using MIST isochrones and supplemented using DSEP isochrones. The observed clusters were then classified based on the Trumpler classification scheme and catalogued.

Additionally, a further 6 clusters of interest were also characterised using MIST isochrones. Each cluster showed resultant parameters that fell within the expected range of their relevant WEBDA study or entry in the collected supplementary data. Any significant invariance due to the lack of definition on the main sequence (Be 28 and Bo 2) and smaller variance as expected due to the fitting of modern isochrones. This method proved to have moderate success in determining cluster parameter with few unexpected discrepancies. The main inaccuracy coming in the form of metallicity estimation near zero. Small variance made distinction difficult to pinpoint where the true value may lie, this task usually falls to spectroscopic surveys of clusters.

The latter part of the study focused on the placement of old open clusters in the milky way as a means to investigate galactic evolution. Inferring from the distribution of open clusters as a function of galactocentric distance there was an underabundance in the inner disk. The main contributor to this underabundance was determined to be destructive dynamical interactions towards the centre of the galactic disk. However, there was still a substantial amount of old and ancient (> 1Gyr) clusters found near the galactic disk. The presence of these clusters suggested a more linked interaction between the internal dynamic of clusters based on their initial mass, the degree of how disruptive the galactic environment and highly elliptical orbits migrating older clusters back towards the core.

It was then finally shown that the cluster population showed a thickening of the outer disk due to the old open clusters through the increase in clusters at an increased Z position.

THIRD PARTY SOFTWARE AND CATALOGS

This work made use of a variety of software suites and python modules. Ginga was used as the primary image viewer and used as reference when performing photmetry. Astropy and associated modules were extensively used. Along with use of pandas to handle dataframes for both isochrone interpolation and data management. Photoutils was used for all photometry related computations. Astroquery was used to to query all catalogs. NumPy and Uncertainties packages were used for both standard computations and error propagation. All statistics implemented in population determination (Standardizing, DBSCAN and HDBSCAN) were handled by Sci-kit learn. Matplotlib were used for all plots. All other modules used as described in the main body of work.

Software:
Astropy (Astropy Collaboration et al. 2018),
Astroquery Ginsburg et al. (2019),
Isochrones (Morton 2015),
Sci-kit Learn (Pedregosa et al. 2011),
Uncertainties (Lebigot 2018),
Pandas (pandas development team 2020),
Photoutils (Bradley et al. 2020),
Matplotlib (Hunter 2007),
NumPy (Harris et al. 2020),
Glob

Catalogues:
APASS9 (Henden et al. 2015)
Gaia DR2 (Gaia Collaboration et al. 2018)
WEBDA (Netopil et al. 2012)

All data and processing files can be found on the author's GitHub.

ACKNOWLEDGMENTS

I would like to give my thanks to Dr Antonio Martin-Carillo for his patience, warmth and depth throughout this project. He made this project an absolute joy from start to finish. I want to give a special thanks to Camin Mac Cionna for his marvellous code, coffee and 'career' advice, to my open cluster partner in crime, Eoin Fitzpatrick, for making my exploration of the universe a little less lonely and to Sean J. Brennan for the wise insights and advice in cycling and astrophysics a-like.

Furthermore, I would like to thank my peers for making the last four years of learning about the cosmos the best experience I've ever had. I wish them every luck and success in their future careers.

To A-a-ron, Ben, Ciara, Cian, Hugh, Joe, Laura, Sharon, and Tiernan, thank you for taking care of me for the past few years. Your friendship is both invaluable and necessary.

Finally, to my family, for their unwavering support and help in the pursuit of my dreams always. Thank you for making all of this possible.

REFERENCES

Agrawal, P., Szécsi, D., Stevenson, S., Eldridge, J. J., & Hurley, J. 2022, MNRAS, 512, 5717, doi: 10.1093/mnras/stac930

Angelo, M. S., Santos, J. F. C., Corradi, W. J. B., & Maia, F. F. S. 2019, A&A, 624, A8, doi: 10.1051/0004-6361/201832702

Asplund, M., Grevesse, N., Sauval, A. J., & Scott, P. 2009, Annual Review of Astronomy and Astrophysics, 47, 481, doi: 10.1146/annurev.astro.46.060407.145222

Astropy Collaboration, Price-Whelan, A. M., Sipőcz, B. M., et al. 2018, AJ, 156, 123, doi: 10.3847/1538-3881/aabc4f

Becker, W., & Fenkart, R. B. 1970, in The Spiral Structure of our Galaxy, ed. W. Becker & G. I. Kontopoulos, Vol. 38, 205

Bevington, P. R., & Robinson, D. K. 2003, Data reduction and error analysis for the physical sciences (Mcgraw Hill)

Bhatt, H., Sagar, R., & Pandey, J. C. 2012, NewA, 17, 160, doi: 10.1016/j.newast.2011.07.015

Bonatto, C., Kerber, L. O., Bica, E., & Santiago, B. X. 2006, A&A, 446, 121, doi: 10.1051/0004-6361:20053573

Bossini, D., Vallenari, A., Bragaglia, A., et al. 2019, A&A, 623, A108, doi: 10.1051/0004-6361/201834693

Bradley, L., Sipőcz, B., Robitaille, T., et al. 2020, astropy/photutils: 1.0.0, 1.0.0, Zenodo, doi: 10.5281/zenodo.4044744

Bressan, A., Marigo, P., Girardi, L., et al. 2012, MNRAS, 427, 127, doi: 10.1111/j.1365-2966.2012.21948.x

Campello, R. J. G. B., Moulavi, D., & Sander, J. 2013, in Advances in Knowledge Discovery and Data Mining, ed. J. Pei, V. S. Tseng, L. Cao, H. Motoda, & G. Xu (Berlin, Heidelberg: Springer Berlin Heidelberg), 160–172

Cantat-Gaudin, T., Anders, F., Castro-Ginard, A., et al. 2020, A&A, 640, A1, doi: 10.1051/0004-6361/202038192

Carraro, G., Chaboyer, B., & Perencevich, J. 2006, MNRAS, 365, 867, doi: 10.1111/j.1365-2966.2005.09762.x

Choi, J., Dotter, A., Conroy, C., et al. 2016, ApJ, 823, 102, doi: 10.3847/0004-637X/823/2/102

de Jager, C., Nieuwenhuijzen, H., & van der Hucht, K. A. 1988, A&AS, 72, 259

Dias, W., Alessi, B., Moitinho, A., & Lépine, J. 2002, Astronomy & Astrophysics, 389, 871

Dotter, A., Chaboyer, B., Jevremović, D., et al. 2008, ApJS, 178, 89, doi: 10.1086/589654

Durgapal, A. K., Pandey, A. K., & Mohan, V. 2001, A&A, 372, 71, doi: 10.1051/0004-6361:20010305

Dyson, J., & Williams, D. 1980, Physics of the Interstellar Medium (Wiley). https://books.google.ie/books?id=XILvAAAAMAAJ

Ester, M., Kriegel, H.-P., Sander, J., & Xu, X. 1996, in (AAAI Press), 226–231

Frandsen, S., & Arentoft, T. 1998, A&A, 333, 524

Gaia Collaboration, Brown, A. G. A., Vallenari, A., et al. 2018, A&A, 616, A1, doi: 10.1051/0004-6361/201833051

Ginsburg, A., Sipőcz, B. M., Brasseur, C. E., et al. 2019, AJ, 157, 98, doi: 10.3847/1538-3881/aafc33

Gravity Collaboration, Abuter, R., Amorim, A., et al. 2019, A&A, 625, L10, doi: 10.1051/0004-6361/201935656

Harris, C. R., Millman, K. J., van der Walt, S. J., et al. 2020, Nature, 585, 357, doi: 10.1038/s41586-020-2649-2

Henden, A. A., Levine, S., Terrell, D., & Welch, D. L. 2015, in American Astronomical Society Meeting Abstracts, Vol. 225, American Astronomical Society Meeting Abstracts #225, 336.16

Herschel, W. 1785, Philosophical Transactions of the Royal Society of London Series I, 75, 213

Herwig, F. 2000, A&A, 360, 952. https://arxiv.org/abs/astro-ph/0007139

Hunter, J. D. 2007, Computing in Science & Engineering, 9, 90, doi: 10.1109/MCSE.2007.55

Janes, K. A., Tilley, C., & Lynga, G. 1988, AJ, 95, 771, doi: 10.1086/114676

Kaliberda, V. S. 1973, Soviet Ast., 16, 837

Kaluzny, J., & Mazur, B. 1991, AcA, 41, 279

Koposov, S. E., Glushkova, E. V., & Zolotukhin, I. Y. 2008, A&A, 486, 771, doi: 10.1051/0004-6361:20078630

Kyeong, J.-M., Byun, Y.-I., & Sung, E.-C. 2001, Journal of Korean Astronomical Society, 34, 143, doi: 10.5303/JKAS.2001.34.3.143

Lata, S., Mohan, V., & Sagar, R. 2004, Bulletin of the Astronomical Society of India, 32, 371

Lebigot, E. O. 2018. http://pythonhosted.org/uncertainties/

Ledoux, P. 1947, ApJ, 105, 305, doi: 10.1086/144905

Lynga, G. 1981, Astronomical Data Center Bulletin, 1, 90

Lynga, G. 1982, Astronomy and Astrophysics, 109, 213

Lyngå, G. 1988, in European Southern Observatory Conference and Workshop Proceedings, Vol. 28, European Southern Observatory Conference and Workshop Proceedings, 379–382

Mohan, V., Bijaoui, A., Creze, M., & Robin, A. C. 1988, Astrophysics and Space Science, 73, 85

Morton, T. D. 2015, isochrones: Stellar model grid package, Astrophysics Source Code Library, record ascl:1503.010. http://ascl.net/1503.010

Netopil, M., Paunzen, E., & Stütz, C. 2012, in Astrophysics and Space Science Proceedings, Vol. 29, Star Clusters in the Era of Large Surveys, 53, doi: 10.1007/978-3-642-22113-2_7

Nugis, T., & Lamers, H. J. G. L. M. 2000, A&A, 360, 227

Oort, J. H. 1950, BAN, 11, 91

Ortolani, S., Bica, E., Barbuy, B., & Zoccali, M. 2005, A&A, 429, 607, doi: 10.1051/0004-6361:20041458

pandas development team, T. 2020, pandas-dev/pandas: Pandas, latest, Zenodo, doi: 10.5281/zenodo.3509134

Paxton, B., Schwab, J., Bauer, E. B., et al. 2018, ApJS, 234, 34, doi: 10.3847/1538-4365/aaa5a8

Pedregosa, F., Varoquaux, G., Gramfort, A., et al. 2011, Journal of Machine Learning Research, 12, 2825

Phelps, R. L., & Janes, K. A. 1994, ApJS, 90, 31, doi: 10.1086/191857

Schilbach, E., Kharchenko, N. V., Piskunov, A. E., Röser, S., & Scholz, R. D. 2006, A&A, 456, 523, doi: 10.1051/0004-6361:20054663

Shapley, H. 1918, ApJ, 48, 154, doi: 10.1086/142423

Spitzer, Lyman, J. 1958, ApJ, 127, 17, doi: 10.1086/146435

Stott, J. J. 2018, A&A, 609, A36, doi: 10.1051/0004-6361/201628568

Trumpler, R. J. 1930, Lick Observatory Bulletin, 420, 154, doi: 10.5479/ADS/bib/1930LicOB.14.154T

Turbide, L., & Moffat, A. F. J. 1993, AJ, 105, 1831, doi: 10.1086/116558

Valle, G., Dell'Omodarme, M., & Tognelli, E. 2021, A&A, 649, A127, doi: 10.1051/0004-6361/202140413

—. 2022, A&A, 658, A141, doi: 10.1051/0004-6361/202142454

van den Bergh, S. 1958, ZA, 46, 176

Vink, J. S., de Koter, A., & Lamers, H. J. G. L. M. 2001, A&A, 369, 574, doi: 10.1051/0004-6361:20010127

APPENDIX

A. SUPPLEMENTARY CLASSIFICATION PLOTS

A.1. *Cluster Images*

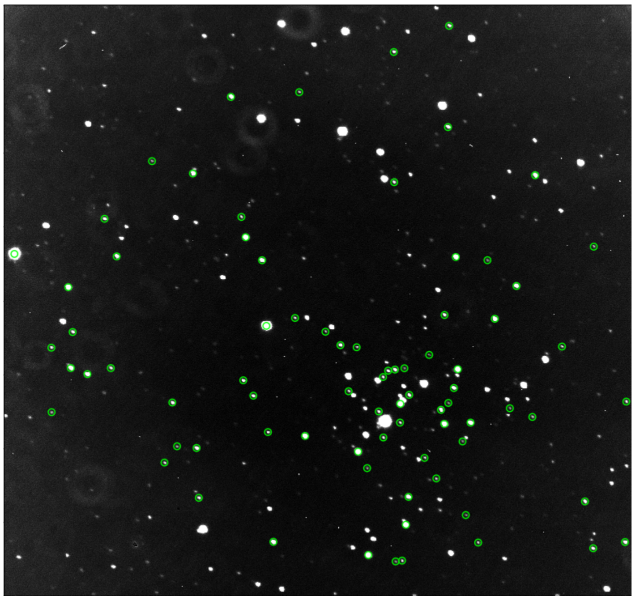

(a) Berkeley 28

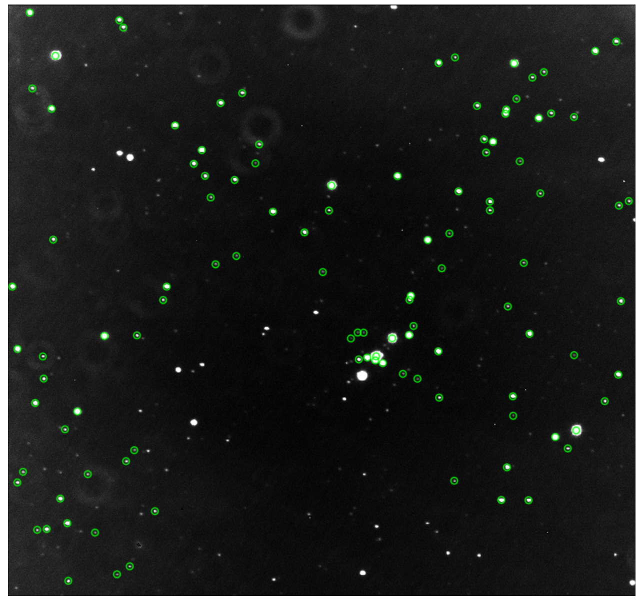

(b) Bochum 2

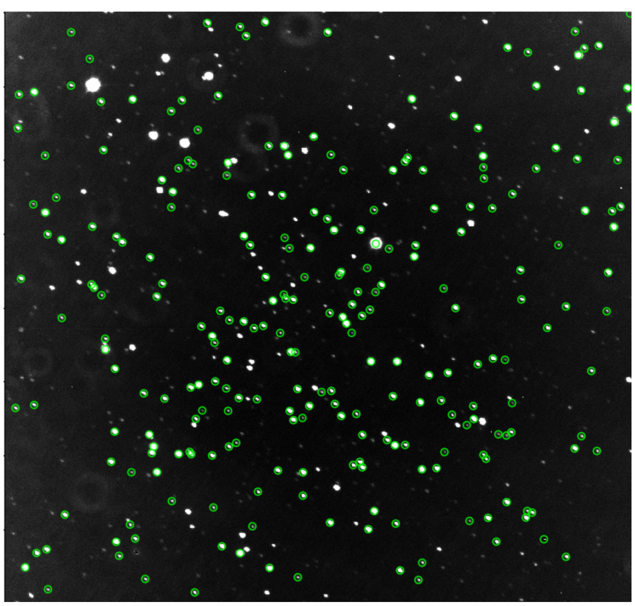

(c) NGC2324

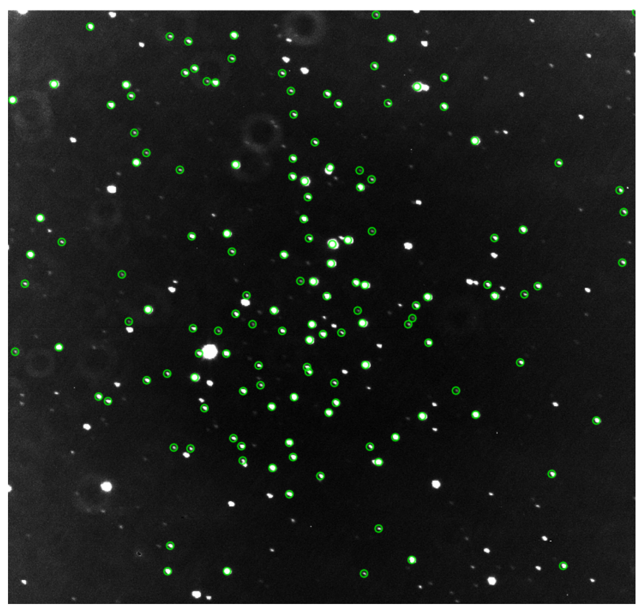

(d) NGC2355

Figure 11. V filter images detailing the 10' by 10' field with each cluster. Each confirmed star is shown by ∘ (lime)

A.2. *Central Separation Distribution*

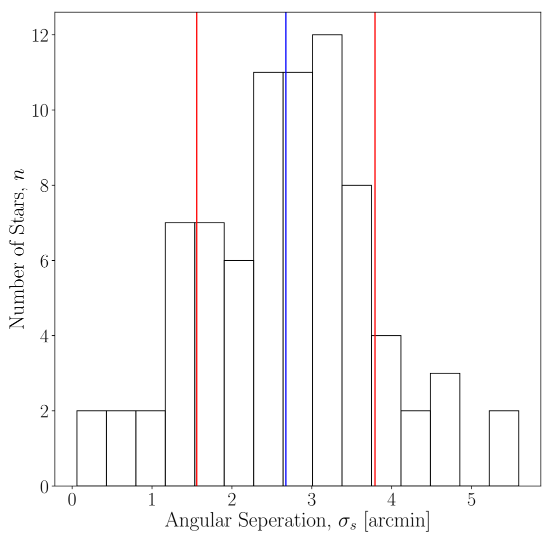

(a) Berkeley 28

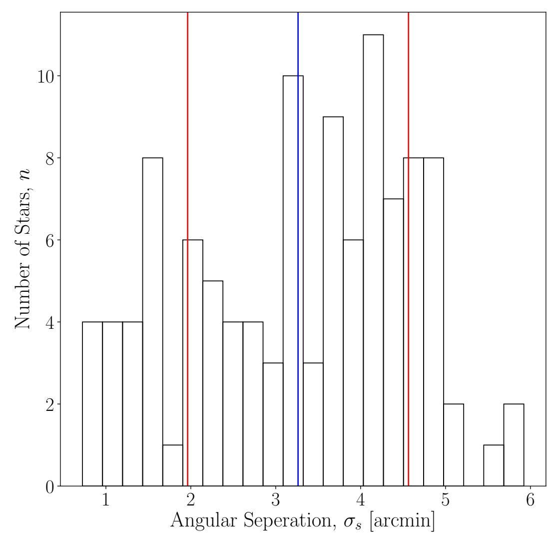

(b) Bochum 2

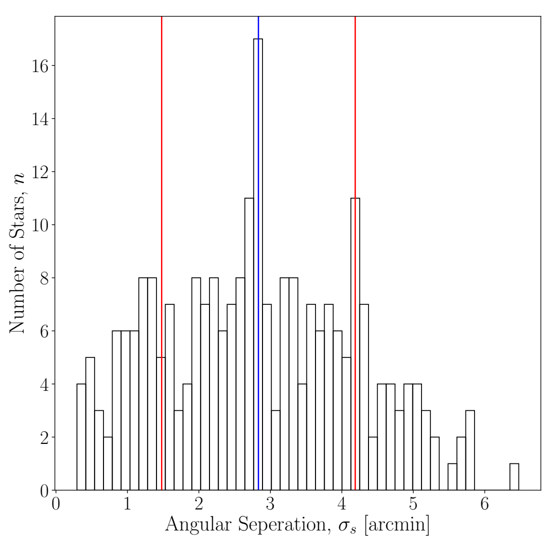

(c) NGC2324

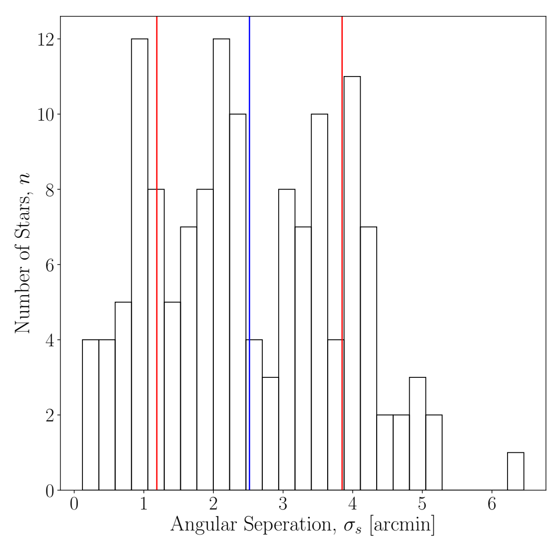

(d) NGC2355

Figure 12. Distribution of angular separation (σ_s) from cluster center (given in table 1). The bin number used in each plot is equivalent to 20% of the population size.x

B. STELLAR CATALOGS

The following four tables detail the magnitudes and location of each of the confirmed stars from each cluster. All ascribed errors were calculated as discussed in the paper's main body.

Table 6. Stellar catalog for Berkeley 28.

no.	RA J2000	DEC J2000	B Magnitude	V Magnitude	BV Magnitude
Population Size: $n = 79$					
1	102.9763	2.8994	17.502 ± 0.2738	16.044 ± 0.1832	1.049 ± 0.2950
2	102.9827	2.9651	19.262 ± 0.3124	16.410 ± 0.1848	2.441 ± 0.3320
3	102.9829	2.9513	18.321 ± 0.2851	16.508 ± 0.1853	1.404 ± 0.3067
4	102.9846	2.8802	17.153 ± 0.2716	15.715 ± 0.1821	1.028 ± 0.2922
5	102.9909	2.9280	17.743 ± 0.2761	16.451 ± 0.1850	0.882 ± 0.2983
6	102.9937	2.9009	18.730 ± 0.2947	16.816 ± 0.1871	1.504 ± 0.3168
7	102.9941	2.9669	16.693 ± 0.2705	15.500 ± 0.1816	0.783 ± 0.2909
8	102.9946	2.9265	18.265 ± 0.2840	16.598 ± 0.1858	1.256 ± 0.3060
9	102.9963	2.9766	16.851 ± 0.2706	15.601 ± 0.1818	0.840 ± 0.2912
10	102.9964	2.9685	16.213 ± 0.2712	15.089 ± 0.1808	0.714 ± 0.2911
11	102.9983	2.9116	18.192 ± 0.2826	16.731 ± 0.1866	1.050 ± 0.3052
12	103.0025	2.9694	17.515 ± 0.2739	15.865 ± 0.1826	1.240 ± 0.2947
13	103.0035	2.9138	18.076 ± 0.2807	16.831 ± 0.1872	0.835 ± 0.3038
14	103.0041	2.9121	17.594 ± 0.2746	16.532 ± 0.1854	0.653 ± 0.2971
15	103.0056	2.8784	17.384 ± 0.2729	15.698 ± 0.1821	1.276 ± 0.2934
16	103.0066	2.9349	16.632 ± 0.2705	15.151 ± 0.1809	1.071 ± 0.2904
17	103.0080	2.9488	18.391 ± 0.2865	16.830 ± 0.1872	1.150 ± 0.3092
18	103.0117	2.8823	18.149 ± 0.2819	16.700 ± 0.1864	1.038 ± 0.3044
19	103.0141	2.9071	17.292 ± 0.2723	16.306 ± 0.1843	0.577 ± 0.2943
20	103.0149	2.9062	18.348 ± 0.2856	16.929 ± 0.1879	1.009 ± 0.3088
21	103.0156	2.9232	15.121 ± 0.2782	14.297 ± 0.1801	0.414 ± 0.2971
22	103.0158	2.9218	17.097 ± 0.2713	16.162 ± 0.1837	0.525 ± 0.2930
23	103.0180	2.9153	18.123 ± 0.2814	17.133 ± 0.1895	0.579 ± 0.3059
24	103.0181	2.9218	17.780 ± 0.2766	16.845 ± 0.1873	0.525 ± 0.3001
25	103.0184	2.9361	17.158 ± 0.2716	16.215 ± 0.1839	0.532 ± 0.2933
26	103.0191	2.9104	14.921 ± 0.2801	13.996 ± 0.1801	0.514 ± 0.2989
27	103.0199	2.9420	16.365 ± 0.2708	15.502 ± 0.1816	0.453 ± 0.2912
28	103.0207	2.8926	16.487 ± 0.2706	15.549 ± 0.1817	0.528 ± 0.2910
29	103.0213	2.8976	18.113 ± 0.2813	16.790 ± 0.1870	0.914 ± 0.3042
30	103.0223	2.9268	17.963 ± 0.2790	17.060 ± 0.1889	0.492 ± 0.3033
31	103.0231	2.9331	17.284 ± 0.2722	16.444 ± 0.1850	0.429 ± 0.2946
32	103.0231	2.9478	18.093 ± 0.2809	16.867 ± 0.1875	0.816 ± 0.3042
33	103.0237	2.9201	14.219 ± 0.2879	12.594 ± 0.1810	1.215 ± 0.3067
34	103.0239	2.9025	17.734 ± 0.2760	16.724 ± 0.1865	0.600 ± 0.2991
35	103.0252	2.8904	17.617 ± 0.2748	16.392 ± 0.1847	0.815 ± 0.2968

Table 6 *continued*

Table 6 *(continued)*

no.	RA J2000	DEC J2000	B Magnitude	V Magnitude	BV Magnitude
36	103.0254	2.9022	16.454 ± 0.2706	15.596 ± 0.1818	0.447 ± 0.2912
37	103.0258	3.0029	17.783 ± 0.2766	15.817 ± 0.1825	1.556 ± 0.2971
38	103.0265	2.9504	16.885 ± 0.2707	15.951 ± 0.1829	0.524 ± 0.2919
39	103.0272	2.9175	16.810 ± 0.2706	15.961 ± 0.1829	0.438 ± 0.2918
40	103.0279	2.8934	15.866 ± 0.2727	14.971 ± 0.1806	0.485 ± 0.2924
41	103.0282	2.9238	18.175 ± 0.2823	17.048 ± 0.1888	0.718 ± 0.3063
42	103.0289	2.9164	15.782 ± 0.2732	14.513 ± 0.1802	0.859 ± 0.2925
43	103.0291	2.9050	16.286 ± 0.2710	15.484 ± 0.1816	0.393 ± 0.2913
44	103.0292	2.8879	17.742 ± 0.2761	15.628 ± 0.1819	1.704 ± 0.2963
45	103.0294	2.9154	14.630 ± 0.2831	13.379 ± 0.1803	0.841 ± 0.3018
46	103.0294	2.9173	16.466 ± 0.2706	15.182 ± 0.1810	0.874 ± 0.2906
47	103.0295	2.9110	17.219 ± 0.2719	16.321 ± 0.1844	0.488 ± 0.2939
48	103.0296	2.9347	17.148 ± 0.2715	16.329 ± 0.1844	0.409 ± 0.2936
49	103.0304	2.9235	17.080 ± 0.2713	16.167 ± 0.1837	0.503 ± 0.2929
50	103.0321	2.9233	17.212 ± 0.2718	16.335 ± 0.1844	0.466 ± 0.2939
51	103.0322	2.8932	17.453 ± 0.2734	16.380 ± 0.1847	0.663 ± 0.2955
52	103.0324	2.9252	17.272 ± 0.2722	16.387 ± 0.1847	0.475 ± 0.2944
53	103.0345	2.9137	17.326 ± 0.2725	16.457 ± 0.1850	0.459 ± 0.2949
54	103.0347	2.9210	14.999 ± 0.2793	13.666 ± 0.1801	0.923 ± 0.2982
55	103.0378	2.9145	16.801 ± 0.2706	15.963 ± 0.1829	0.428 ± 0.2918
56	103.0379	2.8859	16.636 ± 0.2705	15.258 ± 0.1811	0.968 ± 0.2906
57	103.0394	2.9290	17.683 ± 0.2755	16.841 ± 0.1873	0.431 ± 0.2991
58	103.0408	2.9057	17.877 ± 0.2778	16.820 ± 0.1872	0.647 ± 0.3011
59	103.0414	2.8819	16.436 ± 0.2706	15.444 ± 0.1815	0.582 ± 0.2910
60	103.0415	2.9186	17.576 ± 0.2744	16.698 ± 0.1864	0.468 ± 0.2975
61	103.0432	2.9296	16.585 ± 0.2705	15.782 ± 0.1823	0.393 ± 0.2914
62	103.0450	2.9101	17.383 ± 0.2729	16.560 ± 0.1856	0.413 ± 0.2956
63	103.0514	2.9502	17.854 ± 0.2775	16.822 ± 0.1872	0.622 ± 0.3008
64	103.0520	2.9083	15.658 ± 0.2739	14.825 ± 0.1805	0.423 ± 0.2934
65	103.0538	2.9362	17.670 ± 0.2754	16.772 ± 0.1868	0.488 ± 0.2987
66	103.0608	2.9094	17.195 ± 0.2718	16.394 ± 0.1847	0.392 ± 0.2940
67	103.0678	2.9885	16.590 ± 0.2705	15.492 ± 0.1816	0.688 ± 0.2909
68	103.0697	2.9514	17.805 ± 0.2769	16.560 ± 0.1856	0.836 ± 0.2993
69	103.0707	2.9461	16.060 ± 0.2718	15.142 ± 0.1809	0.507 ± 0.2916
70	103.0751	2.8774	17.028 ± 0.2711	15.953 ± 0.1829	0.665 ± 0.2922
71	103.0767	2.9591	17.151 ± 0.2716	16.092 ± 0.1834	0.649 ± 0.2930
72	103.0802	2.9858	17.028 ± 0.2711	15.877 ± 0.1826	0.741 ± 0.2921
73	103.0982	2.8784	17.487 ± 0.2737	15.741 ± 0.1822	1.336 ± 0.2942
74	103.0983	2.9604	17.526 ± 0.2740	15.970 ± 0.1830	1.146 ± 0.2950
75	103.1031	2.9239	16.418 ± 0.2707	15.331 ± 0.1812	0.677 ± 0.2908
76	103.1090	2.8814	17.658 ± 0.2752	16.137 ± 0.1836	1.111 ± 0.2965

Table 6 *continued*

Table 6 *(continued)*

no.	RA J2000	DEC J2000	B Magnitude	V Magnitude	BV Magnitude
77	103.1108	2.9908	17.934 ± 0.2786	16.076 ± 0.1833	1.448 ± 0.2995
78	103.1115	2.9303	18.013 ± 0.2797	16.186 ± 0.1838	1.417 ± 0.3008
79	103.1118	2.9151	18.424 ± 0.2872	16.503 ± 0.1853	1.511 ± 0.3087

Table 7. Stellar catalog for Bochum 2.

no.	RA J2000	DEC J2000	B Magnitude	V Magnitude	BV Magnitude
			Population Size: $n = 110$		
1	102.2901	0.4598	15.185 ± 0.1492	12.420 ± 0.3868	0.142 ± 0.2928
2	102.2691	0.4576	16.705 ± 0.1523	13.484 ± 0.3836	0.597 ± 0.2903
3	102.2682	0.4559	17.453 ± 0.1585	13.930 ± 0.3829	0.899 ± 0.2926
4	102.1521	0.4502	17.539 ± 0.1595	13.683 ± 0.3832	1.231 ± 0.2936
5	102.1571	0.4481	15.259 ± 0.1492	12.545 ± 0.3863	0.090 ± 0.2922
6	102.2843	0.4495	12.280 ± 0.1615	9.724 ± 0.4009	-0.068 ± 0.3173
7	102.1902	0.4473	17.816 ± 0.1631	14.441 ± 0.3826	0.751 ± 0.2948
8	102.1941	0.4460	16.002 ± 0.1496	13.247 ± 0.3841	0.131 ± 0.2896
9	102.1763	0.4456	13.510 ± 0.1545	10.729 ± 0.3948	0.157 ± 0.3060
10	102.1694	0.4434	18.388 ± 0.1731	14.426 ± 0.3826	1.338 ± 0.3005
11	102.1721	0.4421	17.773 ± 0.1625	14.265 ± 0.3827	0.884 ± 0.2945
12	102.2899	0.4419	18.095 ± 0.1675	13.984 ± 0.3828	1.487 ± 0.2976
13	102.2405	0.4399	16.814 ± 0.1530	13.919 ± 0.3829	0.270 ± 0.2897
14	102.1759	0.4372	18.254 ± 0.1705	14.669 ± 0.3828	0.961 ± 0.2991
15	102.2457	0.4376	16.392 ± 0.1508	13.056 ± 0.3847	0.712 ± 0.2909
16	102.1853	0.4357	17.373 ± 0.1577	14.220 ± 0.3827	0.529 ± 0.2919
17	102.2855	0.4370	15.312 ± 0.1491	12.565 ± 0.3862	0.122 ± 0.2921
18	102.1784	0.4347	16.091 ± 0.1498	12.936 ± 0.3850	0.531 ± 0.2908
19	102.1679	0.4336	18.337 ± 0.1721	14.335 ± 0.3826	1.378 ± 0.2999
20	102.1786	0.4337	15.484 ± 0.1491	12.638 ± 0.3860	0.222 ± 0.2917
21	102.1625	0.4326	17.482 ± 0.1589	14.341 ± 0.3826	0.518 ± 0.2925
22	102.1708	0.4325	14.624 ± 0.1503	11.573 ± 0.3904	0.427 ± 0.2982
23	102.2565	0.4326	15.423 ± 0.1491	12.765 ± 0.3855	0.034 ± 0.2912
24	102.1838	0.4278	17.137 ± 0.1554	14.284 ± 0.3827	0.228 ± 0.2906
25	102.1817	0.4272	14.318 ± 0.1512	11.879 ± 0.3890	-0.184 ± 0.2968
26	102.2368	0.4277	17.524 ± 0.1593	14.037 ± 0.3828	0.863 ± 0.2929
27	102.2503	0.4266	15.721 ± 0.1492	12.782 ± 0.3855	0.315 ± 0.2911
28	102.1834	0.4247	17.423 ± 0.1582	14.468 ± 0.3827	0.331 ± 0.2921
29	102.1755	0.4224	18.277 ± 0.1709	14.788 ± 0.3829	0.866 ± 0.2995
30	102.2378	0.4233	18.382 ± 0.1730	15.368 ± 0.3842	0.390 ± 0.3023

Table 7 *continued*

Table 7 *(continued)*

no.	RA J2000	DEC J2000	B Magnitude	V Magnitude	BV Magnitude
31	102.2523	0.4234	16.891 ± 0.1535	13.708 ± 0.3832	0.559 ± 0.2903
32	102.2497	0.4205	17.082 ± 0.1550	14.081 ± 0.3828	0.377 ± 0.2905
33	102.2044	0.4196	14.332 ± 0.1511	11.745 ± 0.3896	-0.038 ± 0.2975
34	102.2428	0.4194	16.774 ± 0.1527	14.155 ± 0.3827	-0.005 ± 0.2893
35	102.2200	0.4177	12.064 ± 0.1630	9.769 ± 0.4006	-0.328 ± 0.3177
36	102.1901	0.4156	16.018 ± 0.1497	13.505 ± 0.3836	-0.111 ± 0.2888
37	102.1708	0.4148	18.012 ± 0.1662	14.737 ± 0.3828	0.651 ± 0.2968
38	102.2485	0.4154	17.952 ± 0.1652	14.828 ± 0.3829	0.500 ± 0.2964
39	102.1500	0.4125	17.880 ± 0.1641	14.464 ± 0.3827	0.793 ± 0.2954
40	102.1828	0.4131	16.559 ± 0.1515	13.836 ± 0.3830	0.099 ± 0.2891
41	102.1524	0.4115	17.899 ± 0.1644	14.517 ± 0.3827	0.758 ± 0.2955
42	102.2207	0.4118	16.983 ± 0.1542	14.517 ± 0.3827	-0.158 ± 0.2900
43	102.1828	0.4110	17.288 ± 0.1568	14.522 ± 0.3827	0.143 ± 0.2914
44	102.2339	0.4118	16.034 ± 0.1497	12.959 ± 0.3849	0.451 ± 0.2907
45	102.2266	0.4068	16.246 ± 0.1503	13.695 ± 0.3832	-0.072 ± 0.2887
46	102.1924	0.4058	18.125 ± 0.1681	15.585 ± 0.3850	-0.084 ± 0.3006
47	102.2858	0.4062	17.075 ± 0.1549	13.957 ± 0.3829	0.494 ± 0.2907
48	102.1976	0.4043	13.949 ± 0.1526	11.353 ± 0.3915	-0.028 ± 0.3007
49	102.2427	0.4015	18.036 ± 0.1665	15.385 ± 0.3842	0.027 ± 0.2988
50	102.1751	0.3984	17.902 ± 0.1644	14.819 ± 0.3829	0.458 ± 0.2959
51	102.2477	0.3996	18.400 ± 0.1734	15.407 ± 0.3843	0.369 ± 0.3027
52	102.1944	0.3976	18.513 ± 0.1758	15.638 ± 0.3852	0.251 ± 0.3053
53	102.2224	0.3973	18.023 ± 0.1663	15.659 ± 0.3853	-0.261 ± 0.3001
54	102.2957	0.3953	15.526 ± 0.1491	12.788 ± 0.3855	0.114 ± 0.2911
55	102.2593	0.3946	15.212 ± 0.1492	12.682 ± 0.3858	-0.094 ± 0.2916
56	102.2018	0.3913	14.409 ± 0.1509	11.890 ± 0.3889	-0.105 ± 0.2966
57	102.2602	0.3915	17.774 ± 0.1625	14.631 ± 0.3827	0.519 ± 0.2946
58	102.2022	0.3903	16.903 ± 0.1536	13.256 ± 0.3841	1.023 ± 0.2916
59	102.1524	0.3889	16.878 ± 0.1534	13.937 ± 0.3829	0.317 ± 0.2899
60	102.1790	0.3883	18.129 ± 0.1681	15.213 ± 0.3837	0.292 ± 0.2990
61	102.2014	0.3841	17.733 ± 0.1620	15.437 ± 0.3844	-0.328 ± 0.2965
62	102.2145	0.3829	18.084 ± 0.1674	16.097 ± 0.3878	-0.637 ± 0.3038
63	102.2131	0.3828	18.138 ± 0.1683	16.029 ± 0.3874	-0.515 ± 0.3038
64	102.1741	0.3817	15.834 ± 0.1493	13.061 ± 0.3846	0.148 ± 0.2901
65	102.2665	0.3833	17.376 ± 0.1577	14.485 ± 0.3827	0.267 ± 0.2919
66	102.2025	0.3820	14.025 ± 0.1523	11.440 ± 0.3911	-0.040 ± 0.3000
67	102.2742	0.3833	13.533 ± 0.1544	11.125 ± 0.3927	-0.217 ± 0.3032
68	102.2162	0.3815	18.002 ± 0.1660	16.262 ± 0.3890	-0.884 ± 0.3047
69	102.2064	0.3814	11.823 ± 0.1646	9.312 ± 0.4035	-0.114 ± 0.3222
70	102.2947	0.3806	15.642 ± 0.1491	12.699 ± 0.3858	0.319 ± 0.2915
71	102.1956	0.3780	15.180 ± 0.1493	12.748 ± 0.3856	-0.192 ± 0.2913

Table 7 *continued*

Table 7 *(continued)*

no.	RA J2000	DEC J2000	B Magnitude	V Magnitude	BV Magnitude
72	102.1637	0.3764	18.260 ± 0.1706	15.092 ± 0.3834	0.544 ± 0.3000
73	102.2103	0.3772	11.434 ± 0.1673	8.879 ± 0.4065	-0.069 ± 0.3273
74	102.2888	0.3787	17.752 ± 0.1622	14.405 ± 0.3826	0.723 ± 0.2943
75	102.2124	0.3769	14.655 ± 0.1502	12.173 ± 0.3877	-0.142 ± 0.2946
76	102.2144	0.3765	16.788 ± 0.1528	14.461 ± 0.3827	-0.297 ± 0.2893
77	102.2105	0.3762	11.434 ± 0.1673	10.333 ± 0.3971	-1.523 ± 0.3156
78	102.2088	0.3755	14.412 ± 0.1509	11.928 ± 0.3888	-0.140 ± 0.2963
79	102.2041	0.3729	17.883 ± 0.1641	15.829 ± 0.3862	-0.569 ± 0.2999
80	102.1534	0.3716	16.239 ± 0.1502	13.518 ± 0.3835	0.097 ± 0.2891
81	102.2887	0.3735	17.374 ± 0.1577	14.159 ± 0.3827	0.591 ± 0.2919
82	102.2007	0.3717	18.063 ± 0.1670	16.047 ± 0.3875	-0.608 ± 0.3032
83	102.1783	0.3671	15.791 ± 0.1493	13.183 ± 0.3843	-0.016 ± 0.2896
84	102.1957	0.3671	16.608 ± 0.1518	14.250 ± 0.3827	-0.266 ± 0.2887
85	102.1567	0.3654	17.533 ± 0.1594	14.543 ± 0.3827	0.366 ± 0.2929
86	102.2908	0.3678	16.208 ± 0.1501	13.308 ± 0.3840	0.276 ± 0.2897
87	102.2809	0.3656	14.121 ± 0.1519	11.626 ± 0.3902	-0.130 ± 0.2986
88	102.1783	0.3625	18.223 ± 0.1699	15.673 ± 0.3854	-0.074 ± 0.3021
89	102.2839	0.3615	17.870 ± 0.1639	14.422 ± 0.3826	0.825 ± 0.2953
90	102.1635	0.3587	11.561 ± 0.1664	9.058 ± 0.4052	-0.121 ± 0.3253
91	102.1685	0.3572	13.625 ± 0.1540	11.300 ± 0.3918	-0.299 ± 0.3018
92	102.1656	0.3545	17.761 ± 0.1624	14.418 ± 0.3826	0.719 ± 0.2944
93	102.2677	0.3562	18.121 ± 0.1680	14.859 ± 0.3830	0.637 ± 0.2980
94	102.2697	0.3537	17.941 ± 0.1650	14.573 ± 0.3827	0.744 ± 0.2959
95	102.1800	0.3503	16.058 ± 0.1497	13.408 ± 0.3838	0.025 ± 0.2891
96	102.2940	0.3516	18.115 ± 0.1679	14.278 ± 0.3827	1.213 ± 0.2975
97	102.2788	0.3508	18.006 ± 0.1661	14.288 ± 0.3827	1.094 ± 0.2965
98	102.1925	0.3475	17.845 ± 0.1636	15.176 ± 0.3836	0.045 ± 0.2963
99	102.2954	0.3492	17.259 ± 0.1565	13.865 ± 0.3830	0.770 ± 0.2917
100	102.2854	0.3452	16.086 ± 0.1498	13.237 ± 0.3842	0.225 ± 0.2897
101	102.1815	0.3427	16.047 ± 0.1497	13.182 ± 0.3843	0.241 ± 0.2898
102	102.1751	0.3425	16.478 ± 0.1512	13.812 ± 0.3830	0.043 ± 0.2889
103	102.2631	0.3418	17.749 ± 0.1622	14.589 ± 0.3827	0.536 ± 0.2944
104	102.2838	0.3393	15.962 ± 0.1495	13.141 ± 0.3844	0.197 ± 0.2899
105	102.2887	0.3381	17.084 ± 0.1550	13.860 ± 0.3830	0.600 ± 0.2908
106	102.2909	0.3379	18.271 ± 0.1708	14.289 ± 0.3827	1.358 ± 0.2991
107	102.2773	0.3370	18.181 ± 0.1691	14.542 ± 0.3827	1.015 ± 0.2982
108	102.2693	0.3289	17.968 ± 0.1654	14.486 ± 0.3827	0.858 ± 0.2961
109	102.2723	0.3271	18.093 ± 0.1675	14.643 ± 0.3827	0.826 ± 0.2974
110	102.2838	0.3258	17.480 ± 0.1588	14.160 ± 0.3827	0.696 ± 0.2926

Table 8. Stellar catalog for NGC 2324.

no.	RA J2000	DEC J2000	B Magnitude	V Magnitude	BV Magnitude
			Population Size: $n = 251$		
1	106.0320	1.0263	16.979 ± 0.2136	16.222 ± 0.1053	-0.308 ± 0.2213
2	105.9987	1.0177	17.434 ± 0.2181	16.054 ± 0.1044	0.314 ± 0.2252
3	106.0556	1.0286	17.084 ± 0.2145	16.007 ± 0.1042	0.011 ± 0.2216
4	106.0382	1.0512	17.094 ± 0.2146	15.944 ± 0.1039	0.084 ± 0.2215
5	105.9826	1.0289	17.342 ± 0.2171	15.849 ± 0.1035	0.428 ± 0.2238
6	106.0143	1.0555	17.057 ± 0.2142	15.835 ± 0.1034	0.156 ± 0.2210
7	106.0161	1.0613	17.110 ± 0.2147	15.825 ± 0.1034	0.219 ± 0.2214
8	106.0291	1.0476	16.778 ± 0.2122	15.814 ± 0.1033	-0.102 ± 0.2190
9	106.0309	1.0594	16.918 ± 0.2131	15.761 ± 0.1031	0.090 ± 0.2198
10	106.0442	1.0013	16.991 ± 0.2137	15.721 ± 0.1029	0.204 ± 0.2202
11	106.0495	1.0284	16.669 ± 0.2116	15.717 ± 0.1029	-0.114 ± 0.2182
12	106.0369	1.0464	16.785 ± 0.2122	15.707 ± 0.1029	0.012 ± 0.2188
13	105.9968	1.0264	16.638 ± 0.2114	15.703 ± 0.1029	-0.131 ± 0.2180
14	105.9931	1.0016	17.073 ± 0.2144	15.692 ± 0.1028	0.315 ± 0.2209
15	106.0407	1.0536	16.925 ± 0.2132	15.667 ± 0.1027	0.192 ± 0.2197
16	106.0274	1.0323	16.767 ± 0.2121	15.667 ± 0.1027	0.034 ± 0.2186
17	106.0336	0.9892	16.787 ± 0.2122	15.572 ± 0.1024	0.148 ± 0.2186
18	106.0542	1.0754	17.463 ± 0.2185	15.559 ± 0.1023	0.838 ± 0.2246
19	106.0313	1.0692	16.783 ± 0.2122	15.554 ± 0.1023	0.162 ± 0.2185
20	105.9841	1.0214	17.096 ± 0.2146	15.509 ± 0.1022	0.522 ± 0.2207
21	106.0528	1.0410	16.584 ± 0.2111	15.473 ± 0.1020	0.045 ± 0.2173
22	106.0193	1.0270	16.304 ± 0.2101	15.447 ± 0.1020	-0.209 ± 0.2163
23	106.0343	1.0663	16.540 ± 0.2109	15.423 ± 0.1019	0.050 ± 0.2171
24	105.9778	0.9913	17.114 ± 0.2147	15.423 ± 0.1019	0.625 ± 0.2208
25	106.0358	1.0662	16.608 ± 0.2112	15.416 ± 0.1019	0.126 ± 0.2174
26	106.0525	1.0444	16.579 ± 0.2111	15.407 ± 0.1018	0.107 ± 0.2172
27	106.0053	0.9881	16.662 ± 0.2115	15.399 ± 0.1018	0.197 ± 0.2176
28	106.0157	1.0514	16.487 ± 0.2107	15.396 ± 0.1018	0.025 ± 0.2168
29	106.0043	0.9921	16.697 ± 0.2117	15.395 ± 0.1018	0.236 ± 0.2178
30	105.9810	0.9939	16.951 ± 0.2134	15.384 ± 0.1018	0.501 ± 0.2194
31	105.9710	1.0659	17.103 ± 0.2146	15.378 ± 0.1017	0.660 ± 0.2206
32	105.9634	1.0453	17.115 ± 0.2147	15.367 ± 0.1017	0.683 ± 0.2207
33	105.9842	1.0098	17.045 ± 0.2141	15.365 ± 0.1017	0.614 ± 0.2201
34	105.9665	1.0210	17.170 ± 0.2153	15.343 ± 0.1016	0.761 ± 0.2212
35	106.0567	1.0868	16.980 ± 0.2136	15.320 ± 0.1016	0.594 ± 0.2195
36	106.0499	1.0336	16.353 ± 0.2102	15.309 ± 0.1015	-0.022 ± 0.2162
37	106.0553	1.0949	17.153 ± 0.2151	15.299 ± 0.1015	0.788 ± 0.2209
38	106.0631	1.0076	17.054 ± 0.2142	15.293 ± 0.1015	0.695 ± 0.2201
39	106.0533	1.0059	16.826 ± 0.2125	15.292 ± 0.1015	0.468 ± 0.2184
40	106.0621	1.0766	16.961 ± 0.2134	15.287 ± 0.1015	0.609 ± 0.2193

Table 8 *continued*

Table 8 *(continued)*

no.	RA J2000	DEC J2000	B Magnitude	V Magnitude	BV Magnitude
41	105.9629	1.0175	17.165 ± 0.2152	15.275 ± 0.1014	0.824 ± 0.2210
42	105.9882	1.0846	16.948 ± 0.2133	15.271 ± 0.1014	0.611 ± 0.2192
43	105.9800	1.0797	17.306 ± 0.2166	15.265 ± 0.1014	0.975 ± 0.2224
44	106.0726	1.0145	17.267 ± 0.2162	15.255 ± 0.1014	0.946 ± 0.2220
45	106.0252	1.0508	16.359 ± 0.2103	15.224 ± 0.1013	0.069 ± 0.2161
46	106.0578	1.0877	17.004 ± 0.2138	15.208 ± 0.1012	0.730 ± 0.2196
47	106.0040	1.0989	17.150 ± 0.2151	15.200 ± 0.1012	0.884 ± 0.2208
48	106.0241	1.0882	16.611 ± 0.2113	15.199 ± 0.1012	0.346 ± 0.2171
49	106.0488	1.0838	17.187 ± 0.2154	15.192 ± 0.1012	0.930 ± 0.2211
50	106.0142	1.0749	16.290 ± 0.2101	15.182 ± 0.1011	0.041 ± 0.2159
51	106.0510	1.0519	16.221 ± 0.2099	15.155 ± 0.1011	0.000 ± 0.2157
52	105.9881	1.0819	16.670 ± 0.2116	15.153 ± 0.1011	0.450 ± 0.2173
53	105.9833	1.0301	16.319 ± 0.2101	15.137 ± 0.1010	0.116 ± 0.2159
54	106.0790	1.0563	16.877 ± 0.2128	15.136 ± 0.1010	0.675 ± 0.2185
55	105.9600	1.0502	17.051 ± 0.2142	15.133 ± 0.1010	0.852 ± 0.2198
56	106.0393	0.9967	16.211 ± 0.2099	15.130 ± 0.1010	0.015 ± 0.2156
57	106.0184	1.0557	16.071 ± 0.2096	15.091 ± 0.1009	-0.087 ± 0.2153
58	105.9890	1.0160	16.734 ± 0.2119	15.082 ± 0.1009	0.585 ± 0.2176
59	106.0212	1.0846	16.200 ± 0.2098	15.080 ± 0.1009	0.054 ± 0.2155
60	106.0489	1.0496	16.100 ± 0.2097	15.072 ± 0.1009	-0.038 ± 0.2154
61	106.0272	0.9848	16.282 ± 0.2100	15.067 ± 0.1008	0.149 ± 0.2157
62	106.0359	1.0554	17.004 ± 0.2138	15.064 ± 0.1008	0.874 ± 0.2194
63	106.0579	0.9862	16.380 ± 0.2103	15.054 ± 0.1008	0.260 ± 0.2160
64	106.0080	1.0195	16.052 ± 0.2096	15.043 ± 0.1008	-0.057 ± 0.2153
65	106.0373	1.0413	15.956 ± 0.2095	15.004 ± 0.1007	-0.114 ± 0.2151
66	106.0495	1.0200	15.988 ± 0.2095	14.992 ± 0.1006	-0.070 ± 0.2151
67	106.0253	1.0730	16.233 ± 0.2099	14.991 ± 0.1006	0.177 ± 0.2155
68	106.0947	1.0782	17.212 ± 0.2157	14.969 ± 0.1006	1.177 ± 0.2211
69	106.0885	1.0511	16.815 ± 0.2124	14.959 ± 0.1006	0.790 ± 0.2179
70	105.9918	1.0284	16.011 ± 0.2096	14.949 ± 0.1005	-0.004 ± 0.2151
71	105.9795	1.0037	16.627 ± 0.2113	14.946 ± 0.1005	0.615 ± 0.2168
72	106.0498	1.1099	16.864 ± 0.2127	14.941 ± 0.1005	0.857 ± 0.2182
73	106.0286	1.0142	15.965 ± 0.2095	14.933 ± 0.1005	-0.034 ± 0.2151
74	106.0892	1.0796	16.981 ± 0.2136	14.931 ± 0.1005	0.983 ± 0.2190
75	106.0203	1.0151	15.862 ± 0.2095	14.914 ± 0.1005	-0.118 ± 0.2150
76	106.0427	1.0309	15.802 ± 0.2095	14.912 ± 0.1005	-0.176 ± 0.2150
77	106.0696	0.9896	16.461 ± 0.2106	14.908 ± 0.1004	0.487 ± 0.2161
78	106.0572	1.0266	15.953 ± 0.2095	14.904 ± 0.1004	-0.017 ± 0.2150
79	106.0735	1.0033	16.656 ± 0.2115	14.899 ± 0.1004	0.691 ± 0.2169
80	106.0926	0.9878	16.976 ± 0.2136	14.882 ± 0.1004	1.028 ± 0.2189
81	106.0505	1.1124	16.674 ± 0.2116	14.872 ± 0.1004	0.736 ± 0.2170

Table 8 *continued*

Table 8 *(continued)*

no.	RA J2000	DEC J2000	B Magnitude	V Magnitude	BV Magnitude
82	105.9830	1.0221	16.010 ± 0.2096	14.862 ± 0.1003	0.081 ± 0.2150
83	105.9863	1.0748	16.194 ± 0.2098	14.859 ± 0.1003	0.269 ± 0.2153
84	106.0783	1.0460	16.616 ± 0.2113	14.858 ± 0.1003	0.691 ± 0.2167
85	106.0198	1.0015	15.927 ± 0.2095	14.844 ± 0.1003	0.017 ± 0.2149
86	105.9758	1.0841	16.436 ± 0.2105	14.843 ± 0.1003	0.527 ± 0.2159
87	106.0525	1.0353	15.834 ± 0.2095	14.827 ± 0.1003	-0.059 ± 0.2149
88	105.9800	1.0532	16.493 ± 0.2107	14.825 ± 0.1003	0.602 ± 0.2161
89	106.0122	1.0208	15.883 ± 0.2095	14.824 ± 0.1002	-0.007 ± 0.2149
90	105.9896	1.0169	16.358 ± 0.2103	14.823 ± 0.1002	0.470 ± 0.2157
91	106.0998	1.0303	17.299 ± 0.2166	14.823 ± 0.1002	1.410 ± 0.2218
92	106.0106	1.0310	15.776 ± 0.2095	14.805 ± 0.1002	-0.095 ± 0.2149
93	106.0762	1.0942	16.805 ± 0.2123	14.799 ± 0.1002	0.939 ± 0.2177
94	105.9695	1.0514	16.129 ± 0.2097	14.795 ± 0.1002	0.269 ± 0.2151
95	106.0243	1.0295	15.678 ± 0.2095	14.791 ± 0.1002	-0.179 ± 0.2149
96	106.0046	1.0664	15.863 ± 0.2095	14.780 ± 0.1002	0.017 ± 0.2149
97	105.9905	1.0382	15.845 ± 0.2095	14.770 ± 0.1001	0.009 ± 0.2148
98	106.0104	1.0013	15.859 ± 0.2095	14.767 ± 0.1001	0.027 ± 0.2148
99	105.9869	0.9967	16.002 ± 0.2095	14.766 ± 0.1001	0.170 ± 0.2149
100	106.0589	1.1020	16.292 ± 0.2101	14.757 ± 0.1001	0.469 ± 0.2541
101	105.9769	1.1117	16.511 ± 0.2108	14.753 ± 0.1001	0.692 ± 0.2161
102	106.0193	1.0993	16.125 ± 0.2097	14.746 ± 0.1001	0.313 ± 0.2150
103	106.0757	0.9951	16.416 ± 0.2104	14.741 ± 0.1001	0.609 ± 0.2158
104	106.0194	1.0640	15.749 ± 0.2095	14.721 ± 0.1000	-0.038 ± 0.2148
105	106.0060	1.0872	16.234 ± 0.2099	14.673 ± 0.0999	0.494 ± 0.2152
106	106.0338	1.0576	15.639 ± 0.2096	14.668 ± 0.0999	-0.095 ± 0.2148
107	105.9565	1.0858	16.366 ± 0.2103	14.664 ± 0.0999	0.636 ± 0.2155
108	105.9657	1.1165	16.697 ± 0.2117	14.644 ± 0.0999	0.987 ± 0.2169
109	106.0116	1.0761	15.666 ± 0.2096	14.642 ± 0.0999	-0.042 ± 0.2148
110	106.0953	1.0309	16.246 ± 0.2099	14.635 ± 0.0998	0.545 ± 0.2152
111	106.0915	1.0710	16.430 ± 0.2105	14.634 ± 0.0998	0.730 ± 0.2157
112	106.0778	1.0906	16.204 ± 0.2099	14.629 ± 0.0998	0.509 ± 0.2151
113	106.0436	1.0672	15.670 ± 0.2096	14.624 ± 0.0998	-0.020 ± 0.2148
114	106.0180	1.0221	15.525 ± 0.2097	14.619 ± 0.0998	-0.160 ± 0.2149
115	106.0387	1.0906	16.355 ± 0.2102	14.612 ± 0.0998	0.677 ± 0.2154
116	105.9582	1.0737	16.554 ± 0.2110	14.596 ± 0.0998	0.892 ± 0.2162
117	105.9915	1.0753	15.752 ± 0.2095	14.593 ± 0.0998	0.094 ± 0.2147
118	106.0355	1.0545	15.793 ± 0.2095	14.582 ± 0.0997	0.145 ± 0.2147
119	106.0694	1.0329	15.904 ± 0.2095	14.581 ± 0.0997	0.257 ± 0.2147
120	106.0980	1.0607	16.513 ± 0.2108	14.570 ± 0.0997	0.877 ± 0.2160
121	106.0975	1.1044	16.797 ± 0.2123	14.561 ± 0.0997	1.171 ± 0.2174
122	106.0845	1.0639	15.955 ± 0.2095	14.551 ± 0.0997	0.338 ± 0.2147

Table 8 *continued*

Table 8 *(continued)*

no.	RA J2000	DEC J2000	B Magnitude	V Magnitude	BV Magnitude
123	106.0555	1.0483	15.617 ± 0.2096	14.543 ± 0.0997	0.008 ± 0.2148
124	106.0585	1.0015	15.800 ± 0.2095	14.537 ± 0.0997	0.197 ± 0.2146
125	106.0358	1.0788	15.611 ± 0.2096	14.530 ± 0.0996	0.015 ± 0.2148
126	105.9800	1.0601	15.710 ± 0.2095	14.529 ± 0.0996	0.115 ± 0.2147
127	106.0781	1.1021	16.475 ± 0.2107	14.526 ± 0.0996	0.883 ± 0.2158
128	106.0187	1.0158	15.570 ± 0.2097	14.518 ± 0.0996	-0.014 ± 0.2148
129	106.0003	0.9951	15.633 ± 0.2096	14.501 ± 0.0996	0.067 ± 0.2147
130	106.0409	1.0481	15.436 ± 0.2099	14.500 ± 0.0996	-0.130 ± 0.2150
131	106.0980	1.0964	16.628 ± 0.2113	14.474 ± 0.0995	1.088 ± 0.2164
132	106.0719	0.9990	15.835 ± 0.2095	14.469 ± 0.0995	0.299 ± 0.2146
133	106.0175	1.0704	15.448 ± 0.2099	14.463 ± 0.0995	-0.081 ± 0.2149
134	106.0884	1.0050	15.960 ± 0.2095	14.458 ± 0.0995	0.436 ± 0.2146
135	105.9741	1.0465	15.628 ± 0.2096	14.442 ± 0.0995	0.120 ± 0.2147
136	106.0433	1.1170	15.850 ± 0.2095	14.421 ± 0.0995	0.363 ± 0.2145
137	106.0517	1.1186	15.792 ± 0.2095	14.383 ± 0.0994	0.343 ± 0.2145
138	106.0503	1.1029	15.714 ± 0.2095	14.383 ± 0.0994	0.266 ± 0.2145
139	106.0129	1.0572	15.346 ± 0.2101	14.368 ± 0.0994	-0.088 ± 0.2151
140	106.0645	1.0586	15.611 ± 0.2096	14.354 ± 0.0993	0.191 ± 0.2146
141	105.9636	1.1125	16.119 ± 0.2097	14.338 ± 0.0993	0.715 ± 0.2147
142	106.0645	1.0316	15.457 ± 0.2098	14.335 ± 0.0993	0.057 ± 0.2148
143	106.0337	1.0542	15.912 ± 0.2095	14.286 ± 0.0992	0.560 ± 0.2144
144	106.0659	1.0556	15.685 ± 0.2095	14.282 ± 0.0992	0.337 ± 0.2145
145	106.0470	1.0313	15.225 ± 0.2104	14.278 ± 0.0992	-0.118 ± 0.2153
146	105.9660	1.0862	15.769 ± 0.2095	14.277 ± 0.0992	0.426 ± 0.2144
147	106.0228	1.0597	16.246 ± 0.2099	14.267 ± 0.0992	0.913 ± 0.2149
148	105.9637	1.0927	15.725 ± 0.2095	14.262 ± 0.0992	0.397 ± 0.2144
149	106.0091	1.1110	16.244 ± 0.2099	14.253 ± 0.0992	0.925 ± 0.2149
150	106.0741	1.0975	15.516 ± 0.2097	14.229 ± 0.0991	0.221 ± 0.2146
151	106.0576	1.0252	15.209 ± 0.2105	14.215 ± 0.0991	-0.073 ± 0.2153
152	106.0334	1.0417	14.215 ± 0.2152	14.203 ± 0.0991	-1.054 ± 0.2199
153	106.0514	0.9968	15.367 ± 0.2100	14.197 ± 0.0991	0.104 ± 0.2149
154	106.0524	1.1203	16.124 ± 0.2097	14.181 ± 0.0991	0.877 ± 0.2146
155	106.0752	1.0700	16.000 ± 0.2095	14.177 ± 0.0991	0.757 ± 0.2144
156	106.0431	1.0650	15.232 ± 0.2104	14.173 ± 0.0991	-0.007 ± 0.2152
157	106.0409	0.9858	15.260 ± 0.2103	14.159 ± 0.0990	0.034 ± 0.2151
158	106.0198	1.0527	15.772 ± 0.2095	14.152 ± 0.0990	0.554 ± 0.2143
159	106.0283	1.0747	15.206 ± 0.2105	14.145 ± 0.0990	-0.005 ± 0.2153
160	106.0535	1.0180	15.221 ± 0.2104	14.139 ± 0.0990	0.016 ± 0.2152
161	106.0385	1.0793	15.161 ± 0.2106	14.085 ± 0.0989	0.010 ± 0.2154
162	106.0024	1.0842	15.254 ± 0.2103	14.078 ± 0.0989	0.110 ± 0.2151
163	106.0465	1.0458	15.084 ± 0.2109	14.071 ± 0.0989	-0.053 ± 0.2156

Table 8 *continued*

Table 8 *(continued)*

no.	RA J2000	DEC J2000	B Magnitude	V Magnitude	BV Magnitude
164	105.9602	1.1131	15.595 ± 0.2096	14.051 ± 0.0989	0.477 ± 0.2144
165	106.0401	1.0596	15.077 ± 0.2109	14.048 ± 0.0989	-0.036 ± 0.2156
166	106.0096	0.9904	15.180 ± 0.2105	14.042 ± 0.0989	0.072 ± 0.2153
167	106.0342	1.0259	14.978 ± 0.2112	14.040 ± 0.0989	-0.128 ± 0.2160
168	105.9843	1.0058	15.159 ± 0.2106	14.017 ± 0.0988	0.076 ± 0.2153
169	106.0588	1.0190	15.894 ± 0.2095	14.014 ± 0.0988	0.814 ± 0.2142
170	106.0842	1.0595	15.297 ± 0.2102	14.001 ± 0.0988	0.230 ± 0.2149
171	106.0761	1.0389	15.148 ± 0.2106	13.993 ± 0.0988	0.089 ± 0.2154
172	105.9799	1.0022	15.113 ± 0.2108	13.989 ± 0.0988	0.058 ± 0.2155
173	106.0738	1.0686	15.215 ± 0.2104	13.969 ± 0.0988	0.181 ± 0.2151
174	106.0007	1.0140	14.970 ± 0.2113	13.963 ± 0.0988	-0.059 ± 0.2160
175	106.0907	1.0583	15.422 ± 0.2099	13.904 ± 0.0987	0.452 ± 0.2146
176	106.0041	1.0138	15.230 ± 0.2104	13.902 ± 0.0987	0.261 ± 0.2151
177	105.9887	1.0022	14.982 ± 0.2112	13.898 ± 0.0987	0.019 ± 0.2159
178	106.0584	1.0184	15.389 ± 0.2100	13.897 ± 0.0987	0.426 ± 0.2147
179	106.0181	1.0145	14.893 ± 0.2116	13.886 ± 0.0987	-0.058 ± 0.2162
180	105.9647	1.1025	15.268 ± 0.2103	13.879 ± 0.0987	0.323 ± 0.2149
181	106.0678	1.0223	15.613 ± 0.2096	13.868 ± 0.0986	0.679 ± 0.2143
182	105.9682	1.0181	14.993 ± 0.2112	13.857 ± 0.0986	0.069 ± 0.2158
183	106.0331	1.0331	14.787 ± 0.2120	13.822 ± 0.0986	-0.101 ± 0.2166
184	105.9976	1.0363	14.834 ± 0.2118	13.814 ± 0.0986	-0.046 ± 0.2164
185	106.0240	1.1174	15.046 ± 0.2110	13.794 ± 0.0985	0.186 ± 0.2156
186	106.0583	1.0340	14.768 ± 0.2121	13.769 ± 0.0985	-0.067 ± 0.2167
187	106.0455	1.0493	14.770 ± 0.2121	13.759 ± 0.0985	-0.055 ± 0.2167
188	106.0000	1.0750	14.826 ± 0.2119	13.745 ± 0.0985	0.015 ± 0.2164
189	105.9948	1.0968	14.911 ± 0.2115	13.723 ± 0.0985	0.122 ± 0.2161
190	106.0439	1.0398	14.733 ± 0.2123	13.706 ± 0.0984	-0.039 ± 0.2168
191	106.0677	1.0189	14.936 ± 0.2114	13.705 ± 0.0984	0.165 ± 0.2159
192	105.9917	1.0253	14.765 ± 0.2121	13.689 ± 0.0984	0.010 ± 0.2167
193	106.0773	1.0171	14.846 ± 0.2118	13.671 ± 0.0984	0.109 ± 0.2163
194	106.0129	1.0222	14.678 ± 0.2126	13.657 ± 0.0984	-0.046 ± 0.2171
195	106.0043	1.0295	14.678 ± 0.2126	13.651 ± 0.0984	-0.039 ± 0.2171
196	106.0304	1.0291	14.696 ± 0.2125	13.646 ± 0.0984	-0.016 ± 0.2170
197	106.0350	1.0280	14.538 ± 0.2133	13.638 ± 0.0984	-0.166 ± 0.2177
198	106.0388	1.1202	15.064 ± 0.2109	13.628 ± 0.0984	0.370 ± 0.2154
199	106.0456	0.9960	14.748 ± 0.2122	13.612 ± 0.0983	0.069 ± 0.2167
200	106.0485	1.0860	16.056 ± 0.2096	13.580 ± 0.0983	1.409 ± 0.2141
201	106.0764	0.9984	14.729 ± 0.2123	13.556 ± 0.0983	0.106 ± 0.2168
202	106.0223	1.0604	14.671 ± 0.2126	13.548 ± 0.0983	0.057 ± 0.2170
203	105.9938	1.0694	14.602 ± 0.2129	13.532 ± 0.0983	0.004 ± 0.2174
204	106.0321	1.0136	14.535 ± 0.2133	13.492 ± 0.0982	-0.023 ± 0.2177

Table 8 *continued*

Table 8 *(continued)*

no.	RA J2000	DEC J2000	B Magnitude	V Magnitude	BV Magnitude
205	106.0443	1.0383	14.500 ± 0.2135	13.482 ± 0.0982	-0.048 ± 0.2179
206	106.0882	1.0696	14.796 ± 0.2120	13.454 ± 0.0982	0.276 ± 0.2164
207	106.0641	1.0832	14.568 ± 0.2131	13.439 ± 0.0982	0.063 ± 0.2175
208	106.0291	1.0333	14.415 ± 0.2140	13.428 ± 0.0982	-0.079 ± 0.2183
209	106.0229	1.0266	14.448 ± 0.2138	13.417 ± 0.0982	-0.035 ± 0.2181
210	106.0020	1.0358	14.424 ± 0.2139	13.358 ± 0.0981	0.000 ± 0.2182
211	106.0593	1.0050	14.422 ± 0.2139	13.260 ± 0.0980	0.096 ± 0.2182
212	106.0706	1.1025	14.610 ± 0.2129	13.235 ± 0.0980	0.310 ± 0.2172
213	106.0496	1.0402	14.225 ± 0.2151	13.233 ± 0.0980	-0.074 ± 0.2194
214	106.0169	1.0001	14.281 ± 0.2147	13.228 ± 0.0980	-0.013 ± 0.2190
215	105.9710	1.0889	14.416 ± 0.2139	13.180 ± 0.0980	0.170 ± 0.2182
216	105.9817	1.1130	14.408 ± 0.2140	13.164 ± 0.0979	0.178 ± 0.2183
217	106.0095	1.0843	14.253 ± 0.2149	13.129 ± 0.0979	0.057 ± 0.2192
218	106.0470	1.0873	14.245 ± 0.2150	13.043 ± 0.0979	0.135 ± 0.2192
219	106.0530	1.0459	14.185 ± 0.2153	13.033 ± 0.0978	0.086 ± 0.2195
220	105.9752	1.1037	14.521 ± 0.2134	13.022 ± 0.0978	0.434 ± 0.2176
221	106.0302	1.0893	14.981 ± 0.2112	12.948 ± 0.0978	0.967 ± 0.2155
222	106.0501	1.0747	14.205 ± 0.2152	12.932 ± 0.0978	0.207 ± 0.2194
223	106.0682	1.0232	14.178 ± 0.2154	12.923 ± 0.0978	0.188 ± 0.2196
224	106.0939	1.1049	14.700 ± 0.2124	12.880 ± 0.0977	0.754 ± 0.2167
225	106.0450	1.0694	13.967 ± 0.2168	12.855 ± 0.0977	0.045 ± 0.2209
226	106.0719	1.0437	13.962 ± 0.2168	12.826 ± 0.0977	0.069 ± 0.2209
227	106.0484	1.0869	14.093 ± 0.2159	12.804 ± 0.0977	0.224 ± 0.2201
228	106.0237	1.0703	13.903 ± 0.2172	12.782 ± 0.0977	0.054 ± 0.2213
229	106.0564	1.0346	14.443 ± 0.2138	12.780 ± 0.0977	0.598 ± 0.2179
230	106.0243	1.0098	14.401 ± 0.2140	12.779 ± 0.0977	0.556 ± 0.2182
231	106.0213	1.0483	13.877 ± 0.2174	12.756 ± 0.0977	0.055 ± 0.2215
232	106.0221	1.0498	14.312 ± 0.2146	12.620 ± 0.0976	0.626 ± 0.2187
233	106.0979	0.9930	13.864 ± 0.2175	12.610 ± 0.0976	0.188 ± 0.2216
234	106.0155	1.0043	14.250 ± 0.2149	12.585 ± 0.0976	0.599 ± 0.2190
235	106.0294	1.0663	13.773 ± 0.2182	12.579 ± 0.0976	0.128 ± 0.2222
236	106.0385	1.0540	13.705 ± 0.2187	12.529 ± 0.0975	0.110 ± 0.2227
237	105.9645	1.0739	13.698 ± 0.2187	12.514 ± 0.0975	0.118 ± 0.2227
238	106.0665	1.0144	13.736 ± 0.2185	12.505 ± 0.0975	0.165 ± 0.2225
239	106.0648	1.0807	13.682 ± 0.2189	12.495 ± 0.0975	0.121 ± 0.2229
240	106.0614	1.0185	14.168 ± 0.2155	12.446 ± 0.0975	0.656 ± 0.2195
241	106.0046	1.1011	14.186 ± 0.2153	12.445 ± 0.0975	0.675 ± 0.2194
242	106.0342	1.0884	14.151 ± 0.2156	12.413 ± 0.0975	0.673 ± 0.2196
243	106.0104	1.0195	13.443 ± 0.2207	12.381 ± 0.0975	-0.004 ± 0.2247
244	105.9915	1.0714	14.050 ± 0.2162	12.311 ± 0.0974	0.674 ± 0.2202
245	105.9882	1.0872	13.186 ± 0.2229	12.028 ± 0.0973	0.092 ± 0.2267

Table 8 *continued*

Table 8 *(continued)*

no.	RA J2000	DEC J2000	B Magnitude	V Magnitude	BV Magnitude
246	105.9898	1.0247	13.183 ± 0.2229	11.917 ± 0.0973	0.201 ± 0.2267
247	105.9651	1.1109	13.741 ± 0.2184	11.812 ± 0.0973	0.863 ± 0.2223
248	106.0157	1.0393	13.167 ± 0.2230	11.787 ± 0.0973	0.314 ± 0.2268
249	105.9571	1.0948	13.300 ± 0.2219	11.776 ± 0.0973	0.458 ± 0.2257
250	106.0672	1.0204	13.436 ± 0.2208	11.528 ± 0.0972	0.842 ± 0.2246
251	106.0140	1.0670	10.760 ± 0.2476	9.315 ± 0.0971	0.380 ± 0.2510

Table 9. Stellar catalog for NGC 2355.

no.	RA J2000	DEC J2000	B Magnitude	V Magnitude	BV Magnitude
Population Size: $n = 139$					
1	109.2294	13.8266	17.683 ± 0.1034	16.254 ± 0.1852	1.428 ± 0.2121
2	109.1918	13.8246	17.368 ± 0.0989	16.045 ± 0.1852	1.323 ± 0.2100
3	109.2639	13.8225	14.607 ± 0.0829	14.137 ± 0.1910	0.469 ± 0.2082
4	109.2795	13.8225	17.392 ± 0.0992	16.087 ± 0.1852	1.305 ± 0.2101
5	109.2258	13.8211	14.306 ± 0.0827	13.845 ± 0.1926	0.462 ± 0.2096
6	109.2508	13.8211	17.023 ± 0.0949	15.785 ± 0.1854	1.237 ± 0.2083
7	109.2180	13.8197	15.253 ± 0.0841	14.689 ± 0.1884	0.564 ± 0.2063
8	109.2517	13.8167	14.884 ± 0.0833	14.397 ± 0.1897	0.487 ± 0.2072
9	109.2737	13.8150	15.911 ± 0.0865	15.173 ± 0.1867	0.738 ± 0.2058
10	109.2473	13.8140	14.199 ± 0.0827	13.742 ± 0.1931	0.457 ± 0.2101
11	109.2525	13.8134	17.175 ± 0.0965	16.238 ± 0.1852	0.937 ± 0.2089
12	109.2133	13.8117	16.296 ± 0.0887	15.605 ± 0.1857	0.691 ± 0.2058
13	109.2707	13.8119	17.506 ± 0.1008	16.258 ± 0.1852	1.248 ± 0.2108
14	109.2687	13.8116	15.439 ± 0.0846	14.819 ± 0.1879	0.620 ± 0.2061
15	109.3078	13.8121	13.460 ± 0.0830	12.921 ± 0.1983	0.539 ± 0.2150
16	109.2903	13.8115	14.063 ± 0.0827	13.608 ± 0.1939	0.455 ± 0.2108
17	109.2199	13.8097	13.035 ± 0.0836	12.081 ± 0.2044	0.954 ± 0.2209
18	109.2181	13.8095	14.352 ± 0.0827	13.834 ± 0.1926	0.518 ± 0.2096
19	109.2417	13.8084	16.569 ± 0.0907	15.870 ± 0.1853	0.699 ± 0.2063
20	109.1948	13.8075	16.909 ± 0.0937	15.780 ± 0.1854	1.128 ± 0.2077
21	109.3178	13.8087	14.426 ± 0.0827	13.895 ± 0.1923	0.531 ± 0.2093
22	109.2270	13.8060	16.986 ± 0.0945	16.092 ± 0.1852	0.894 ± 0.2079
23	109.2391	13.8061	16.064 ± 0.0873	15.464 ± 0.1860	0.600 ± 0.2054
24	109.2941	13.8069	15.555 ± 0.0850	14.926 ± 0.1875	0.630 ± 0.2059
25	109.2135	13.8050	15.694 ± 0.0855	15.056 ± 0.1871	0.638 ± 0.2057
26	109.2499	13.8038	16.772 ± 0.0924	16.132 ± 0.1852	0.641 ± 0.2070
27	109.1806	13.8021	16.644 ± 0.0913	15.797 ± 0.1854	0.848 ± 0.2067

Table 9 *continued*

Table 9 *(continued)*

no.	RA J2000	DEC J2000	B Magnitude	V Magnitude	BV Magnitude
28	109.3036	13.7990	15.822 ± 0.0861	15.150 ± 0.1868	0.672 ± 0.2057
29	109.2449	13.7972	16.469 ± 0.0899	16.006 ± 0.1852	0.464 ± 0.2059
30	109.2857	13.7956	17.470 ± 0.1003	16.392 ± 0.1853	1.078 ± 0.2107
31	109.2503	13.7935	15.711 ± 0.0856	15.231 ± 0.1865	0.480 ± 0.2052
32	109.2883	13.7934	14.192 ± 0.0827	13.715 ± 0.1933	0.478 ± 0.2102
33	109.1861	13.7914	16.995 ± 0.0946	16.049 ± 0.1852	0.946 ± 0.2079
34	109.2643	13.7924	13.585 ± 0.0829	13.132 ± 0.1969	0.453 ± 0.2137
35	109.2414	13.7913	15.797 ± 0.0860	14.550 ± 0.1890	1.247 ± 0.2076
36	109.2778	13.7914	17.308 ± 0.0981	16.480 ± 0.1854	0.828 ± 0.2098
37	109.2420	13.7905	14.400 ± 0.0827	13.491 ± 0.1946	0.908 ± 0.2115
38	109.2506	13.7893	15.381 ± 0.0844	14.938 ± 0.1875	0.443 ± 0.2056
39	109.2403	13.7888	17.546 ± 0.1013	17.057 ± 0.1869	0.489 ± 0.2126
40	109.2476	13.7882	13.121 ± 0.0834	12.206 ± 0.2035	0.915 ± 0.2199
41	109.2342	13.7865	14.303 ± 0.0827	13.890 ± 0.1923	0.413 ± 0.2093
42	109.2945	13.7873	13.192 ± 0.0833	12.739 ± 0.1996	0.453 ± 0.2163
43	109.2469	13.7845	15.903 ± 0.0865	15.500 ± 0.1859	0.404 ± 0.2050
44	109.2204	13.7827	15.656 ± 0.0854	15.210 ± 0.1866	0.446 ± 0.2052
45	109.2700	13.7807	17.000 ± 0.0946	16.474 ± 0.1854	0.526 ± 0.2081
46	109.2481	13.7794	15.048 ± 0.0836	14.696 ± 0.1884	0.352 ± 0.2061
47	109.1951	13.7760	15.303 ± 0.0842	14.806 ± 0.1880	0.497 ± 0.2060
48	109.3096	13.7779	17.478 ± 0.1004	16.175 ± 0.1852	1.303 ± 0.2106
49	109.2667	13.7763	13.665 ± 0.0828	13.239 ± 0.1962	0.426 ± 0.2130
50	109.2752	13.7759	15.723 ± 0.0857	15.252 ± 0.1865	0.471 ± 0.2052
51	109.2393	13.7749	16.474 ± 0.0900	15.847 ± 0.1853	0.627 ± 0.2060
52	109.2021	13.7742	16.066 ± 0.0873	15.557 ± 0.1858	0.509 ± 0.2053
53	109.2375	13.7742	13.553 ± 0.0829	12.660 ± 0.2002	0.892 ± 0.2167
54	109.3066	13.7752	17.518 ± 0.1009	16.285 ± 0.1852	1.233 ± 0.2109
55	109.2413	13.7734	12.548 ± 0.0845	11.540 ± 0.2087	1.008 ± 0.2251
56	109.2232	13.7727	13.425 ± 0.0830	12.955 ± 0.1981	0.470 ± 0.2148
57	109.3143	13.7725	14.809 ± 0.0831	14.318 ± 0.1901	0.491 ± 0.2075
58	109.2531	13.7711	14.700 ± 0.0830	14.277 ± 0.1903	0.423 ± 0.2076
59	109.2025	13.7701	15.132 ± 0.0838	14.679 ± 0.1885	0.453 ± 0.2062
60	109.2418	13.7688	13.208 ± 0.0833	12.742 ± 0.1996	0.466 ± 0.2163
61	109.2923	13.7673	17.634 ± 0.1026	16.627 ± 0.1856	1.007 ± 0.2121
62	109.2796	13.7654	17.191 ± 0.0967	16.399 ± 0.1853	0.792 ± 0.2090
63	109.2461	13.7647	13.735 ± 0.0828	12.754 ± 0.1995	0.981 ± 0.2160
64	109.2086	13.7640	14.817 ± 0.0832	14.424 ± 0.1896	0.393 ± 0.2070
65	109.2070	13.7638	16.044 ± 0.0872	15.456 ± 0.1860	0.588 ± 0.2054
66	109.2337	13.7637	14.025 ± 0.0827	13.070 ± 0.1973	0.955 ± 0.2139
67	109.2041	13.7633	16.427 ± 0.0896	15.935 ± 0.1853	0.493 ± 0.2058
68	109.1919	13.7628	16.108 ± 0.0876	15.519 ± 0.1858	0.589 ± 0.2054

Table 9 *continued*

Table 9 *(continued)*

no.	RA J2000	DEC J2000	B Magnitude	V Magnitude	BV Magnitude
69	109.2007	13.7624	16.336 ± 0.0890	15.818 ± 0.1854	0.518 ± 0.2056
70	109.2623	13.7618	17.051 ± 0.0952	16.498 ± 0.1854	0.553 ± 0.2084
71	109.2429	13.7612	14.883 ± 0.0833	14.457 ± 0.1894	0.426 ± 0.2069
72	109.2024	13.7606	14.282 ± 0.0827	13.832 ± 0.1926	0.450 ± 0.2096
73	109.2186	13.7606	13.723 ± 0.0828	13.290 ± 0.1959	0.433 ± 0.2127
74	109.2627	13.7601	13.585 ± 0.0829	13.114 ± 0.1970	0.471 ± 0.2138
75	109.2861	13.7589	13.311 ± 0.0832	12.889 ± 0.1986	0.423 ± 0.2153
76	109.2558	13.7581	14.005 ± 0.0827	13.606 ± 0.1939	0.399 ± 0.2108
77	109.2355	13.7577	17.514 ± 0.1009	17.200 ± 0.1876	0.314 ± 0.2130
78	109.2650	13.7575	16.270 ± 0.0885	15.960 ± 0.1852	0.310 ± 0.2053
79	109.2438	13.7562	17.032 ± 0.0950	16.678 ± 0.1857	0.354 ± 0.2086
80	109.2908	13.7562	17.589 ± 0.1020	16.743 ± 0.1859	0.846 ± 0.2120
81	109.2345	13.7548	13.616 ± 0.0829	12.736 ± 0.1996	0.880 ± 0.2161
82	109.2610	13.7550	17.328 ± 0.0984	17.198 ± 0.1875	0.130 ± 0.2118
83	109.2467	13.7547	14.290 ± 0.0827	13.740 ± 0.1932	0.550 ± 0.2101
84	109.2234	13.7543	17.218 ± 0.0971	17.043 ± 0.1869	0.176 ± 0.2106
85	109.2415	13.7542	16.081 ± 0.0874	15.787 ± 0.1854	0.294 ± 0.2050
86	109.2908	13.7544	14.898 ± 0.0833	14.488 ± 0.1893	0.409 ± 0.2068
87	109.2539	13.7533	16.259 ± 0.0885	15.949 ± 0.1852	0.310 ± 0.2053
88	109.2396	13.7526	16.630 ± 0.0912	16.369 ± 0.1853	0.261 ± 0.2065
89	109.2441	13.7524	15.190 ± 0.0839	14.852 ± 0.1878	0.338 ± 0.2057
90	109.2473	13.7511	13.366 ± 0.0831	12.924 ± 0.1983	0.442 ± 0.2150
91	109.2186	13.7499	15.515 ± 0.0849	15.165 ± 0.1867	0.349 ± 0.2051
92	109.2307	13.7494	16.090 ± 0.0875	15.736 ± 0.1855	0.355 ± 0.2051
93	109.3184	13.7498	17.980 ± 0.1084	16.176 ± 0.1852	1.804 ± 0.2146
94	109.2716	13.7488	10.659 ± 0.0897	9.542 ± 0.2260	1.118 ± 0.2431
95	109.2675	13.7482	15.219 ± 0.0840	14.854 ± 0.1878	0.365 ± 0.2057
96	109.1966	13.7450	16.823 ± 0.0929	16.239 ± 0.1852	0.584 ± 0.2072
97	109.2597	13.7453	16.464 ± 0.0899	16.248 ± 0.1852	0.215 ± 0.2059
98	109.2340	13.7450	13.333 ± 0.0831	12.895 ± 0.1985	0.438 ± 0.2152
99	109.2481	13.7447	15.982 ± 0.0869	15.564 ± 0.1857	0.418 ± 0.2051
100	109.2477	13.7436	15.836 ± 0.0862	15.375 ± 0.1862	0.461 ± 0.2051
101	109.2392	13.7435	15.697 ± 0.0855	15.409 ± 0.1861	0.288 ± 0.2048
102	109.2752	13.7428	13.203 ± 0.0833	12.786 ± 0.1993	0.417 ± 0.2160
103	109.2868	13.7424	16.540 ± 0.0905	16.024 ± 0.1852	0.516 ± 0.2061
104	109.2717	13.7414	14.645 ± 0.0829	14.300 ± 0.1902	0.345 ± 0.2075
105	109.2940	13.7416	15.941 ± 0.0867	15.270 ± 0.1864	0.671 ± 0.2056
106	109.2334	13.7395	17.122 ± 0.0959	16.900 ± 0.1863	0.222 ± 0.2096
107	109.2636	13.7394	16.039 ± 0.0872	15.754 ± 0.1854	0.286 ± 0.2049
108	109.3086	13.7398	17.399 ± 0.0993	16.271 ± 0.1852	1.128 ± 0.2102
109	109.2514	13.7377	14.396 ± 0.0827	14.051 ± 0.1914	0.345 ± 0.2085

Table 9 *continued*

Table 9 *(continued)*

no.	RA J2000	DEC J2000	B Magnitude	V Magnitude	BV Magnitude
110	109.2738	13.7374	15.967 ± 0.0868	15.600 ± 0.1857	0.367 ± 0.2050
111	109.2413	13.7362	15.210 ± 0.0839	14.871 ± 0.1877	0.339 ± 0.2056
112	109.2177	13.7355	16.633 ± 0.0912	16.259 ± 0.1852	0.374 ± 0.2064
113	109.2730	13.7355	16.496 ± 0.0901	16.122 ± 0.1852	0.374 ± 0.2059
114	109.2431	13.7339	14.399 ± 0.0827	13.994 ± 0.1917	0.405 ± 0.2088
115	109.2077	13.7329	14.514 ± 0.0828	14.111 ± 0.1911	0.402 ± 0.2083
116	109.2206	13.7327	13.630 ± 0.0829	13.198 ± 0.1965	0.432 ± 0.2132
117	109.1786	13.7311	15.513 ± 0.0848	14.994 ± 0.1873	0.519 ± 0.2056
118	109.3015	13.7317	14.513 ± 0.0828	14.109 ± 0.1911	0.404 ± 0.2083
119	109.2662	13.7283	16.167 ± 0.0879	15.906 ± 0.1853	0.262 ± 0.2051
120	109.2527	13.7271	14.708 ± 0.0830	14.401 ± 0.1897	0.308 ± 0.2071
121	109.2643	13.7265	15.965 ± 0.0868	15.692 ± 0.1855	0.273 ± 0.2048
122	109.2333	13.7258	16.488 ± 0.0901	16.248 ± 0.1852	0.240 ± 0.2059
123	109.2806	13.7264	17.161 ± 0.0964	16.634 ± 0.1857	0.527 ± 0.2092
124	109.2766	13.7261	17.091 ± 0.0956	16.487 ± 0.1854	0.604 ± 0.2086
125	109.3051	13.7259	17.741 ± 0.1043	16.422 ± 0.1853	1.319 ± 0.2127
126	109.2640	13.7231	16.892 ± 0.0935	16.048 ± 0.1852	0.843 ± 0.2075
127	109.2323	13.7222	15.016 ± 0.0835	14.329 ± 0.1900	0.688 ± 0.2076
128	109.2637	13.7221	15.978 ± 0.0869	15.524 ± 0.1858	0.454 ± 0.2051
129	109.1896	13.7187	15.811 ± 0.0860	15.240 ± 0.1865	0.571 ± 0.2054
130	109.2454	13.7191	16.323 ± 0.0889	15.965 ± 0.1852	0.358 ± 0.2055
131	109.2457	13.7181	17.399 ± 0.0993	16.875 ± 0.1863	0.525 ± 0.2111
132	109.2579	13.7147	15.539 ± 0.0849	15.148 ± 0.1868	0.391 ± 0.2052
133	109.1919	13.7036	16.181 ± 0.0880	15.638 ± 0.1856	0.543 ± 0.2054
134	109.2575	13.7019	17.211 ± 0.0970	16.815 ± 0.1861	0.396 ± 0.2098
135	109.1874	13.6971	15.858 ± 0.0863	15.334 ± 0.1863	0.525 ± 0.2053
136	109.2094	13.6971	17.624 ± 0.1025	16.730 ± 0.1859	0.894 ± 0.2122
137	109.2683	13.6971	13.973 ± 0.0827	13.616 ± 0.1939	0.357 ± 0.2108
138	109.2354	13.6960	17.038 ± 0.0950	16.550 ± 0.1855	0.488 ± 0.2084
139	109.1808	13.6937	16.758 ± 0.0923	15.946 ± 0.1852	0.812 ± 0.2070

Draft version January 20, 2022
Typeset using LaTeX default style in AASTeX63

Literature Review: Man shoot at something, nothing sure to hit it. A review of Open Clusters, associated CCD Photometry Methodology and their contribution to Stellar and Galatic Evolution

Owen Johnson

(Received January 20, 2022)

Submitted to Dr. Antonio Martin-Carrillo

ABSTRACT

Open clusters are an integral instrument in an astronomers toolbox. They have proven to be one of the most valuable tools in determining the structure and evolution in the Milky Way, acting as stellar and galactic laboratories. They provide insight into astronomical phenomenon such as nuclear synthesis to stellar composition. In this review, basic background information and context is provided to illustrate open clusters place in astronomy. This review also details the methods and means by which science can be performed—using photometry to obtain colour-magnitude diagrams (CMDs) to analyse and survey missing for three open clusters of varying age in the Open Star Cluster Survey and WEBDA catalogues.

Completing a survey of an open cluster can be defined as a cluster classification by determination of reddening, distance and metallicity of clusters. This can be done by means of fitting theoretical isochrones to CMDs to obtain these parameters accurately. This will allow for discussion about the stellar evolution in a given cluster. In the case of an older observed cluster, an investigation into the mass function of white dwarfs can be conducted. In the case of younger clusters, an inquiry can be made into the convection overshooting among the stellar population.

In a circumstantial case, profiling of the sampled clusters spatial distribution would allow for an observation on galactic tracing as open clusters are commonly used as path-finders to find the shape of the Milky Way.

1. INTRODUCTION & BACKGROUND

Clusters of stars are one of the most readily available 'laboratories' to give insight into many Astrophysical phenomena. Study and analysis of clusters lend themselves to the development of theories in the stellar and galactic evolution, along with an insight into the stellar composition and nuclear synthesis but have been used across many fields in astrophysics.

Open clusters are classified based on their sparseness with some distinction about their core, with a higher density usually observed towards their centre, with subcategories within classified open clusters. (Trumpler 1930) Presently, there are about 3000 open clusters in known catalogues with much larger projection for open cluster discoverers on account of Gaia's observations. (Castro-Ginard et al. 2020) This review intends to briefly explain the use of open clusters in explaining stellar evolution and how this can be furthermore extended to galactic evolution. It will also outline some specific details about the questions photometry of open clusters can answer.

2. USING OPEN CLUSTERS AS STELLAR LABORATORIES

Cluster's form the perfect environment for large scale laboratories. This initially became prevalent when examining the colour-magnitude diagrams of open clusters. Stars in the same cluster were found to often have similar properties across the populations (Trumpler 1930) allowing for details of the molecular cloud to hold true for detailed observations. So when an HR diagram is plotted for an open cluster, the stellar population will mainly reside along the main sequence. The use of HR diagrams is how information about stellar evolution is inferred from observational data and, as we will later see, how photometry can be used to make further contributions to stellar and galactic evolution.

2.1. *Colour Magnitude Diagram*

Colour magnitude diagrams (CMDs) are imperative to the study of open clusters. They reveal the evolutionary state of the cluster and information about its stellar constituents. Such as the frequency of binaries, the existence of anomalous stars and the nature of a cluster's mass and luminosity functions. It also provides the reddening, distance and metallicity of clusters. An example of a CMD of an open cluster is illustrated in figure 1, where the main sequence and evolutionary track are distinct.

2.2. *Theoretical Isochrones*

Stellar Isochrones are commonly used date open clusters as the stellar population is around the same age. If the initial mass function of a cluster is well described, the entire observed population can be used to see how the population will evolve over time, given the calculation of isochrone at varying dates (i.e Gyr isochrone in steps of about 0.5 Gyr)[1]. Over the years, many databases have been built up for varying types of clusters. An example of such a database is provided by the Spanish Virtual Observatory[2] with many theoretical isochrones are fed data from near-infrared surveys like 2MASS[3] and UKIDSS[4] to provide more accurate results when comparing to experimental data. See Janes et al. (1988) §II and III for a well-illustrated use of a theoretical isochrone to enhance photometric data. The power of theoretical isochrone is also illustrated in figure 1 where a modified 5 Gyr isochrone is used to estimate the age of Messier 67 (M67).

2.2.1. *Implication of using CMDs on Open Clusters*

The use of CMDs does not come without its challenges, especially when looking at the extremes of the age distributions of open clusters as this project intends to do. When looking at open clusters, especially older ones, the spatial profile can be quite sparse. Due to this, the main sequence, when plotted on a CMD, can be subjected to masking or 'confusion' due to a popular field population. Gozzoli et al. (1996) came up with a remedy for this by means of limiting the field to the most central regions of the cluster. In doing this, further clarity was found in the main sequence. Even in doing this, the main sequence is dominated by the field in comparison to the cluster. Method of de-convolution can be used to resolve this issue further but is noted to be extremely difficult. It involves statistical subtraction by sampling the nearby field that can be used as a comparison against the sample set. This method has its own limitations, mainly that open clusters have distant members from their centre by definition. Once again, there is a commonly used solution to solve this issue by simulating the clusters evolutionary sequence and then comparing theoretical isochrones with the synthetically simulated CMD. (Gozzoli et al. 1996)
The very young open clusters do not get away from their own challenges in obtaining CMDs. As many stars are just entering the main sequence, there can be quite a broad foot on the approach from brighter luminosities. There can also be variable reddening as stars leave the main sequence, which must be subsequently accounted for during analysis. For very young clusters for decent data collection, multiple wavelength observations are required, mainly infrared (IR) and Hα wavelengths are commonly used. (Slesnick et al. 2002) Young clusters also fall victim to embedded nebulosity[5] which lead back into the aforementioned issue with sparsity as seen with older clusters.
In all cases, classification of sparse clusters can be quite difficult unless precise data can be calculated on radial velocity and motion.

3. USING OPEN CLUSTERS FOR GALACTIC TRACING

Observing the Milkyway's shape has always been difficult as the only observation point is from within it. Open clusters are commonly used as path-finders, especially when trying to determine the evolution of the galactic core. Open clusters are of use for determining attributes of the galaxy based on their properties and spatial distribution. It can provide context for a given point or trajectory in galactic evolution. van den Bergh (1958) found that cluster age and location correlated, that the older clusters in the sample size were at a greater distance from the galactic plane from younger, more conventional clusters. This was further added upon in studies by van den Bergh & McClure (1980) where larger sample size was used to determine that clusters with age greater than 1 Gyr were found primarily in the galaxy anti-centre compared to the younger populations of clusters. As time progressed and further studies

[1] *Note:* Steps used to illustrate point this usually isn't the case.
[2] http://svo2.cab.inta-csic.es/theory/iso3/
[3] https://irsa.ipac.caltech.edu/Missions/2mass.html
[4] https://www2.le.ac.uk/departments/physics/research/xroa/astronomical-facilities-1/ukidss
[5] 'Nebulosity' is a term used to describe when a cluster has similar to a nebula such as cloud-like properties.

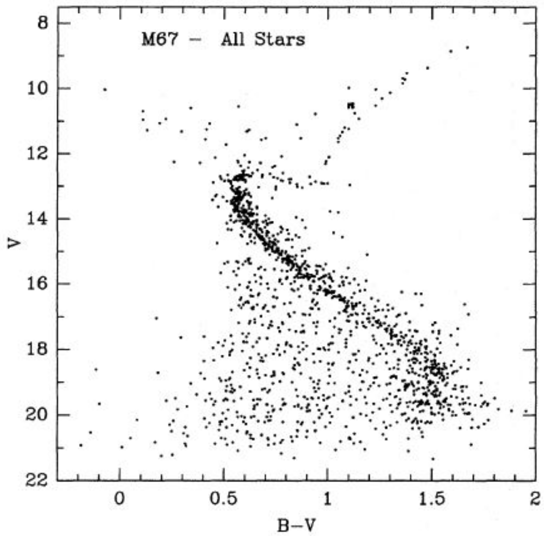

(a) V vs $B-V$ color magnitude diagram of all M67 stars brighter than 12. This CMD exhibits a clear main sequence track.

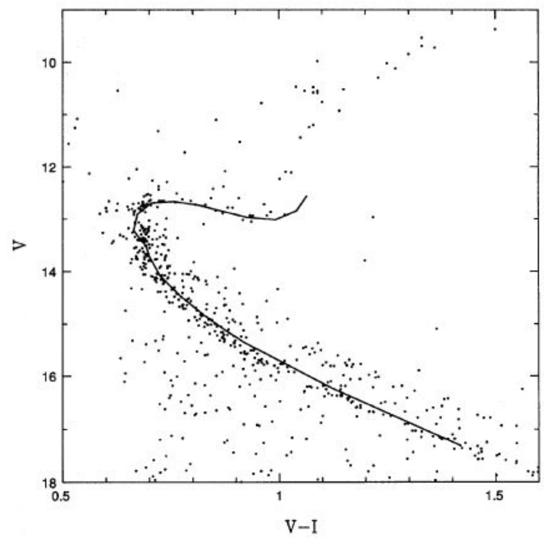

(b) V vs $V-I$ color magnitude diagram of all M67 stars with a distance modulus greater than 9.6. Fitted with a 5 billion year old isochrone for comparison.

Figure 1: Example color magnitude diagrams of of open cluster Messier 67 (M67) produced through photometry by Montgomery et al. (1990). M67 is considered a prime exampled of an 'old' super-cluster with an estimated age of just over ≈ 4 billion years.

were complete, it became apparent that the age of the clusters would see towards the anti-centre of the galactic core. Recent studies in tandem with Gaia data release 2 (DR2) have been using Galactic tracing to infer information about the shape of the Milky Way, specifically the spiral arms. This had been extensively studied by Castro-Ginard et al. (2021). Studies involving galactic tracing require larger sample sizes of clusters in specific locations in the galactic plane, but if target clusters are chosen with the current databases in mind, further precision on cluster parameters can help improve established models and provide an extension to the data garnered by the project.

4. INTENDED PHOTOMETRY METHODOLOGIES

4.1. *Classification of Open Clusters*

When performing analysis, it is important to know the classification of an open cluster. The most common system for doing this was coined by Robert Trumpler, who determined that an open cluster could be classified based on three factors. ***(a)*** Range of brightness, ***(b)*** degree of concentration and ***(c)*** star population in a cluster.

Range of Brightness	**Degree of Concentration**	**Cluster population**
1 - Majority of stellar objects show similar brightness.	I - Strong central concentration (Detached)	p - Poor ($n < 50$)
2 - Moderate brightness ranges between stellar objects.	II - Little central concentration (Detached)	m - Medium ($50 < n < 100$)
3 - Both bright and feint stellar objects	III - No disenable concentration	r - Rich ($n > 100$)
	IV - Clusters not well detached (Strong field concentration)	

Table 1: Details relating to the classification of open clusters as described by the Trumpson classification system. Where n denotes the amounts the stellar population in a given cluster. For example Pleiades is a I3rn cluster and Hyades is a II3m cluster. Where the 'n' flag on a classification relates if the cluster shows nebulosity. (Trumpler 1930; Nilakshi et al. 2002)

4.2. *Photometry*

When approaching photometry regarding open clusters, there is a common theme in methodology with small variations depending on the specific outcomes of a given project. Generally, most open clusters can be sufficiently observed with a telescope around 1 m with observations using U, B, V and I required. Typically exposures in the U, B, V and I are around 600, 600, 300 and 120 seconds, respectively, but the source determines this number and other variables such as weather, so detailed discussion is not possible until further in the project. Typically more frames are taken towards the cluster's core as the stellar objects are less discernible from each other and require more observation to ensure correct classification. Crawford & Perry (1966) and subsequent studies outline in detail the methodology for observing open clusters using photometry with only distinguishable revisions coming in the form of data-analysis and correction methods.

From a practical standpoint, observations will need to be taken over the course of three nights as described by Kalirai et al. (2003) with accumulative combined exposures. CCD image reduction will need to be performed as traditionally done with photometry inclusive of flat-fields, bias and darks. The data will also need to be transformed to calibrate the data (see §§ 5.1 and 5.2 of ??). It will also be imperative to estimate the zero points of observed targets and ensure that estimated uncertainties are in line with that of used catalogues throughout observations.

4.3. *Existing Catalogues & Survey's*

There have been many initiatives to catalogue open clusters throughout the years. In the case of cataloguing open clusters, the conditions for membership must be well defined and understood as they directly change ideas about stellar and galactic evolution. As time progresses, the realms in which these conditions are defined become less transparent. The catalogue of interest in the context of this project will be WEBDA[6]

5. PROPOSED OBSERVATIONS & SCIENTIFIC RELEVANCE

During this project, an ideal case would be to obtain at least three open clusters at the extremes of their lifespan. One rich young open cluster. One open cluster in the middle of its lifespan which exhibits a detached centre with a medium to rich population and one older cluster with at least moderate brightness and distinction about the core. The reason for this desiring targets of these parameters is for many reasons. Mainly due to consideration of the points outlined in **??** section 2. While observing targets on the extremes of their ageing spectrum, it is important to balance the issues this carries. Having a CMD of an open cluster in its infancy may be perfect in theory for analysis on various related problems but is no good if the main sequence cannot be clearly and accurately distinguished within this project's scope.

5.1. *Convective Overshooting*

The inner convective zone and the outer radiative zone can often be subjected to boundary overshooting in stars that are of masses of $2 - 2.5\ M_{\odot}$. The implication of this is that the mass of the core of the stellar object can increase substantially. In turn, this can cause a distinct change in morphology of the produced HR diagram of open clusters surveys outlined that this can happen in clusters from around 600 Myr to several Gyr. This, in turn, causes overestimation in the parameters inferred from CMDs. Thus it's another factor that should be considered when modelling and deriving stellar evolution and cluster age. The effect this had on data obtained from M67 is in-depth discussed in VandenBerg & Stetson (2004).

5.2. *White Dwarfs and the Initial–Final Mass Function*

An attractive faucet for older open cluster observations is their insight into the behaviour of white dwarfs. Open clusters have been used to constrain ranges of parameters of white dwarfs further. Mainly their cooling ages and their upper mass limits in the production of white dwarfs. This provides information about mass loss during the process of stellar evolution and, in turn, lends itself to the study of models that describe galactic chemical evolution and the chemical enrichment of the interstellar medium. Surveys and studies by Kalirai et al. (2003) to present has explored these factories in great depth and provided production of white dwarfs found in the observed old cluster the data could be fitted to proposed models.

[6] https://webda.physics.muni.cz/

5.3. *Aims & Desires*

As with any field in astronomy, the study of open clusters is disadvantaged by a lack of data. Observing and storing raw data for each cluster is a cumbersome task. Furthermore, accurately cataloguing and determining these attributes can be a time-intensive task with many open clusters lacking appropriate observation time with present technology. The versatility and implications of the study of open clusters have been briefly touched on throughout this review. A survey of open clusters in itself can be a career-long undertaking, and the study of stellar and galactic evolution from this even more so. A project that adequately surveys a set of open clusters that may have an inconcise or incomplete parameter database by lack of consideration of implications, as mentioned earlier, would be the overall aim. Any extensions or investigations into stellar or galactic evolution as described above would be a welcome addition.

REFERENCES

Castro-Ginard, A., Jordi, C., Luri, X., et al. 2020, A&A, 635, A45, doi: 10.1051/0004-6361/201937386

Castro-Ginard, A., McMillan, P. J., Luri, X., et al. 2021, A&A, 652, A162, doi: 10.1051/0004-6361/202039751

Crawford, D. L., & Perry, C. L. 1966, AJ, 71, 206, doi: 10.1086/109907

Gozzoli, E., Tosi, M., Marconi, G., & Bragaglia, A. 1996, MNRAS, 283, 66, doi: 10.1093/mnras/283.1.66

Janes, K. A., Tilley, C., & Lynga, G. 1988, AJ, 95, 771, doi: 10.1086/114676

Kalirai, J. S., Fahlman, G. G., Richer, H. B., & Ventura, P. 2003, AJ, 126, 1402, doi: 10.1086/377320

Montgomery, K., Marschall, L., & Janes, K. A. 1990, in Bulletin of the American Astronomical Society, Vol. 22, 1288

Nilakshi, Sagar, R., Pandey, A. K., & Mohan, V. 2002, Astronomy & Astrophysics, 383, 153–162, doi: 10.1051/0004-6361:20011719

Slesnick, C. L., Hillenbrand, L. A., & Massey, P. 2002, ApJ, 576, 880, doi: 10.1086/341865

Trumpler, R. 1930, Lick Observatory Bulletins, 14, 154–188, doi: 10.5479/ads/bib/1930licob.14.154t

van den Bergh, S. 1958, The Astronomical Journal, 63, 492, doi: 10.1086/107816

van den Bergh, S., & McClure, R. D. 1980, A&A, 88, 360

VandenBerg, D. A., & Stetson, P. B. 2004, 116, 997, doi: 10.1086/426340

Data Analysis Report on Open Clusters

Owen Johnson[1]

[1] *University College Dublin, UCD*

1. INTRODUCTION

Open clusters have been shown to be instrumental laboratories to explore many forms of astronomy. However, conducting analysis first requires a linear structure before more in-depth details can be explored. Figure 1 gives a brief overview of the sequence the data analysis for open-cluster science should be carried out. With each outlined step following standard practices from similar studies.

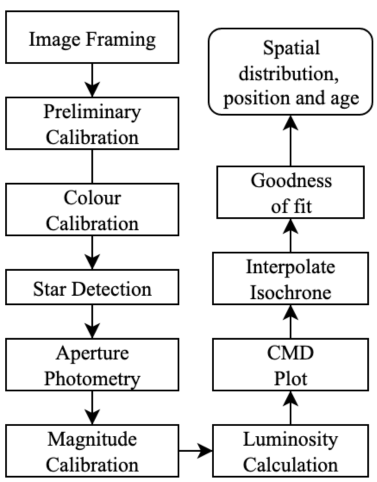

Figure 1. Overview of steps to be carried out during data analysis.

2. PRELIMINARY CALIBRATION

The conventional calibration will be carried out using flat and bias images as with all photometry. However, it is also important to consider the frame size and colour calibration. The use of the telescope at Calor Alto Observatory (CAO) for this project will make use of B, V and R filters, which means that only 50mm of the 100mm detector can be used. This leaves an observable 11' circular unvignetted frame that will need to be cropped before analysis using `numpy.s_`.
This means that about a 10' by 10' area will be suitable for observation after the crop. This will limit the size of the open cluster that can be observed and will need to be taken into consideration when choosing targets.
Color calibration is not as important to consider throughout this study as it aims to be self-contained regarding colour comparison to both experimental and archived data. However, if colour calibration proves to be a necessary step, CAO is equipped with a filter wheel reference sheet along with reference targets. [1]

3. STELLAR DETECTION

Upon first observing open clusters, each member of the clusters must be first identified. After each target has been successfully framed and reduced photometry must be performed to identify each star.
This can be completed using `DAOstarfinder` from the `photutils` python module.[2]
This operates on the DAOFIND algorithm coined by Stetson (1987). When given a threshold value `DAO` will search local density maxima for peaks that surpass this threshold. `DAO` will then fit a 2D Gaussian kernel to find objects of similar shape and size. Furthermore, the applied Gaussian kernel can be used to find the centroid and roundness by marginally fitting a 1D distribution of the Gaussian kernel to the unconvolved data image. The important return of data from the star finder is the x and y centroid positions and roundness.
Once this is complete, it is then possible to continue on the path to magnitude calculation. For a comprehensive discussion of implementation and mathematical framework, see (Howell 2006, Ch. 5.1-5.3) and Stetson (1987)

3.1. *Selecting Detection Parameters*

The two important parameters that require attention is the `threshold` and the `FWHM`.
I. The threshold determines what count number is considered the background and what count number is considered a star.
This value will depend on how noisy the image is so to ensure that they are no false detections the threshold expressed as follow,

$$\texttt{threshold} = 5 \cdot n_{\text{background}} \tag{1}$$

II. The full width at half maximum (FWHM) of the Gaussian distribution defines the resolution of a point source. FWHM is the diameter of the star's image area where intensity has fallen by half its peak value. For

[1] http://w3.caha.es/CAHA/Instruments/CAFOS/cafos22.html
[2] https://github.com/astropy/photutils/tree/v0.3

accurate photometry at FWHM of at least two pixels is required. Where FWHM is initially taken to be 7 to find a hand full of stars. These stars can be fitted to a 2D Gaussian to find FWHM. The FWHM is updated accordingly, and the process is repeated until the desired result is attained. Where FWHM of distribution is expressed as,

$$\mathrm{FWHM} = 2\sqrt{2\ln(2)} \cdot \sigma \quad (2)$$

4. INSTRUMENTAL MAGNITUDE CALIBRATION

4.1. *Instrumental Apparant Magnitude Calaculation*

Next is the measurement of the brightness of each detected source. This is completed using `aperture.photometry` from `photoutils`[3]. The basic idea is that the counts measured can be directly related to magnitude. This is done by sampling a specified aperture area around each detected source along with taking the background counts around the source by defining the bounds of the annulus (Bradley et al. 2020).

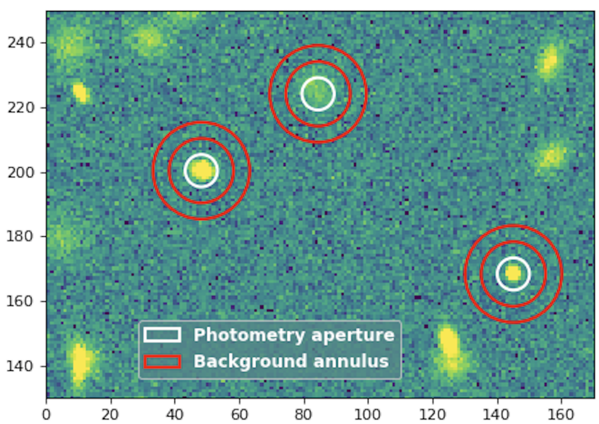

Figure 2. Apertures using `photutils`. White circle is the aperture where the counts are summed and the red annulus is where the background counts are summed. Image curtsey of Bradley et al. (2020)

The number of measured counts from `aperture` photometry is related to magnitude as follows,

$$m_{\mathrm{std}} = -2.5\log_{10} F + \mathrm{ZP} \quad (3)$$

Where m_{std}, is the calibrated magnitude of a given source in the *standard* system. F, is the background-subtracted counts from a given source, and ZP is the zero point of an image.

4.2. *Insturmental Conversion*

Figure 2 shows how `aperture` handles the aperture and annulus. The aperture value is selected based on what aperture returns the lowest signal to noise ratio (SNR) during calibration. This is done by selecting a star from a frame and sampling other stars around it within a defined radius, i.e. 8 arcmins. This group of stars is then queried to a database (i.e. APASS[4]). To return stars from the selected group with the most accurate astrometric values. The varying aperture values are used to see which returns the lowest SNR. A good guess value, in this case, would be the FWHM that was previously determined. The least noisy aperture will be returned and used for subsequent analysis.

The annulus will be selected based on where a uniform background count can be attained, usually around taken with the inner and outer boundary taken as 5 and 10 pixels extended outside the aperture.
In the case where there is an overlapping of stars, the background count can be taken from a sparsely populated region of the frame. This can be easily implemented using `numpy.s_` and `for` loops in tandem with source detection.

Even though the magnitude of the sources can be calculated, they are only instrumentally apparent magnitudes. The next step is to covert each detected target into the standard photometric system. The purpose in this is to negate any discrepancies between the instrumental system and the standard system. This is done through the calculation of the zero point, ZP.

To find the zero-point, the use of reference stars is needed. A plot can be made between instrumental magnitude against the photometric magnitude to find the zero-point (Budding & Demircan 2007, Ch. 6.1) of the system, see fig. 3. If done correctly, all-instrumental bias will be minimised. This procedure needs to be repeated for each filter used.
When the reference stars have been identified eq. (3) can be re-arranged to calculate the zeropoint,

$$\mathrm{ZP} = m_{\mathrm{std}} + 2.5\log_{10} F \quad (4)$$

4.3. *Statistical Uncertainty*

Photon's on a CCD obey a Poission distribution therefore before any measurements or analysis are made there is a built in uncertainty. This uncertainty is commonly referred to as signal to noise ratio (SNR). This is sim-

[3] https://photutils.readthedocs.io

[4] https://www.aavso.org/apass

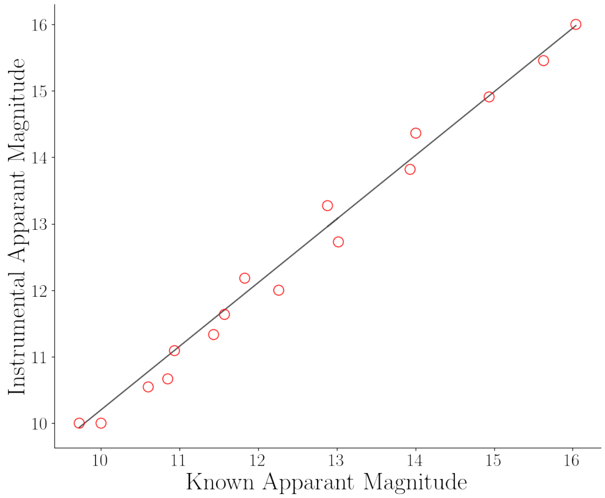

Figure 3. Example plot of Magnitude calibration. Using provided data from NGC3286 and `astroquery` to use SIMBAD magnitude values.

ply the signal from the detected star over the noise in the signal itself (Budding & Demircan 2007, Ch. 5.3). Where it is expressed as follows,

$$n = n_{\text{aperture}} \left(1 + \frac{n_{\text{aperture}}}{n_{\text{annulus}}}\right) \tag{5}$$

$$\text{SNR} = \frac{S_{\text{star}}}{\sqrt{S_{\text{star}} + n\left(S_{\text{bkg}}\right)}} \tag{6}$$

Where n is respective area of pixels and S is the respective photon count. This allows for an error estimation on magnitude to be expressed as follows,

$$\Delta m \sim \frac{1}{\text{SNR}} \tag{7}$$

4.4. *Luminosity and Distance Calculations*

Following ZP being determined, the calculation of distance and luminosity can be determined using the following equations.

$$d = 10^P; \quad P = \frac{5 - m_{\text{std}} - \text{ZP}}{5} \tag{8}$$

Where luminosity can be calculated as follows,

$$L = 4\pi d^2 F \tag{9}$$

An inquiry can also be made into the mass of main-sequence stars present in the stellar population if required by using the following equation.

$$L = L_{\odot} \left(\frac{m}{m_{\odot}}\right)^a \quad (3 \lesssim a \lesssim 4) \tag{10}$$

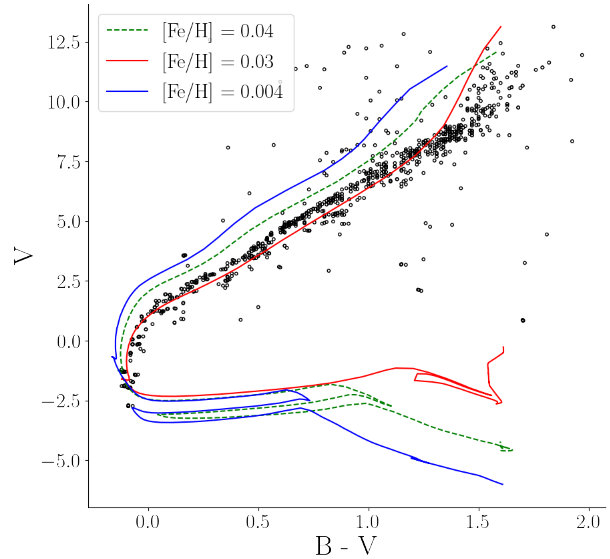

Figure 4. Example CMD plot of M45 using discussed methods using SIMBAD data. MIST isochrones were generated for a range of metallicities between $0.008 < [\text{Fe/H}] < 0.03$. 100 Myr fitted the data closely and parameters are within close range of Vandenberg (1985). All mention packages and databases are used in the creation of this plot as a proof of concept.

5. COLOUR-MAGNITUDE DIAGRAM

Colour magnitude diagrams (CMD) are a variant of Hertzsprung-Russell (HR) diagrams. The HR diagram will summarise the temperatures against magnitudes of the stellar populations, whereas CMDs is magnitude against colour. CMDs are much easier to plot as the CMD does not require the temperature of each star in a cluster. Instead, the ratio of two spectral bands intensity is used. This ratio is directly related to the black body function and related to temperature. The balance is usually expressed as the magnitude difference between two optical spectral bands, i.e. B-V. This can be similarly expanded to flux as it is easier to plot and measure flux in a standard optical spectral band (usually V). Due to this reason, CMDs are used more commonly in cluster observation. See fig. 4 as an example.

Plotting a CMD is relativity easy once proper calibration of magnitudes for the required filters has been performed. It just requires the use of `matplotlib`.

6. THEORTICAL STELLAR ISOCHRONE

Once the CMD has been plotted, it is time to turn to fit a stellar isochrone. This part of the analysis is inferred from much of the information about a stellar population. There are a considerable amount of models for creating isochrones such as MIST[5] (Choi et al. 2016; Paxton et al. 2018).

`isochrone`[6] can be used in tandem with MIST to quickly generate isochrones with varying parameters. This is done using the `StarModel` object class, allowing tabulated pairs of varying parameters to be quickly downloaded in mass to a binary form using the `grid` extension of `starmodel`. `isochrone` uses grid interpolation based on `pandas` and `scipy` modules to produce multi-indexed isochrone data frames at fast speeds. This allows for isochrone model generation and plotting in a more efficient way than a manual generation through MIST and ultimately will allow for a different range of parameters to be fitted due to ease of use and automation of interpolating process.

Parameter	Inferred from Photometry
RA (J2000)	YES
DEC (J2000)	YES
Galaxy Longitude	YES
Galaxy Latitude	YES
Distance	YES
Distance Modulus (m_{std})	YES
Age	YES
Metallicity	ESTIMATED
Reddening	ESTIMATED

Table 1. Required parameters in calculation of a MIST theortical isochrone. YES - can be directly inferred from observations. ESTIMATED - inferral is possible but will have to be compared with other databases.

6.1. *Reddening*

Reddening is a direct result of propagation through the interstellar medium (ISM), causing light to diffuse. The extent of reddening is inversely proportional to the wavelength of the optical light. Reddening can be expressed as an excess of colour, $E(B-V)$ in a photometric system. With this absorption expressed as follows at a given wavelength,

$$A_v = R_v \; E(B-V) \tag{11}$$

Where A_v is the adsorption value at R_v is the degree of redding at a specific wavelength. Reddening will affect the stars' horizontal position when plotting the CMD as the diffuse through the ISM will decrease detected light.

[5] http://waps.cfa.harvard.edu/MIST/references.html

[6] https://isochrones.readthedocs.io/en/latest/

In correcting reddening, the loss of light will be taken into consideration. V-band adsorption, R_v, has been estimated to be ~ 2.5 towards the Milkey Way's bulge (Nataf et al. 2013). However, this value changes based on the target position. Nevertheless, there are plentiful high-resolution spectroscopic studies to provide reliable estimations.

6.2. *Metallicity Esitmations*

Metallicity proves to be quite useful when analysing open clusters as its it's a strong indicator to what stars are part of the stellar population in the cluster itself. Using discrepencies in magnitude along with comparison with metallicity 'imposter' stars can be idenitifed. However, metallicity primarly uses spectorscopy for accurate estimations, commonly analayesd through comparioson of the Sun using a log scale,

$$\left[\frac{\mathrm{Fe}}{\mathrm{H}}\right] = \log_{10}\left[\frac{\mathrm{Fe/H}}{\mathrm{Fe/H}_{\odot}}\right] \tag{12}$$

Using this scale, photometric colours can be used to estimate metallicity to a reasonable degree, as shown by Karaali et al. (2011) using U, V and B filters. However, this would require the use of narrowband filters for more significant periods of observation time to attain values equivalent to high-resolution spectroscopic databases such as Tojeiro et al. (2009).

6.3. *Convection Overshooting*

Convection overshooting has been shown to be a necessary consideration for stellar models which has been most notable shown by VandenBerg & Stetson (2004). It is the also the reason why earlier stellar studies assumed that convection cores were enlarged at some given pressure height. When creating a mdoel convection cores should not exceed $r_{\max}$. The maximum size of a convection core is given as follows as,

$$\int^{r_{\max}} (L_{\mathrm{rad}} - L)\frac{1}{T^2}\frac{dT}{dr}\, dr = 0 \tag{13}$$

Successfully correcting for overshooting produced more accurate plots for the later stages in the main sequence as shown in fig. 5. Most theoretical isochrone models readily include convection overshooting as a parameter, thus making for easier implementation onto CMD plots. Inclusion will see better fits in the later main-sequence as shown by fig. 5 and fig. 4

7. 'GOODNESS' OF ISOCHRONE FIT

In fitting the isochrone to observed data also requires a tangible way to show that the isochrone is well fitted. This is important, especially when dealing with minor

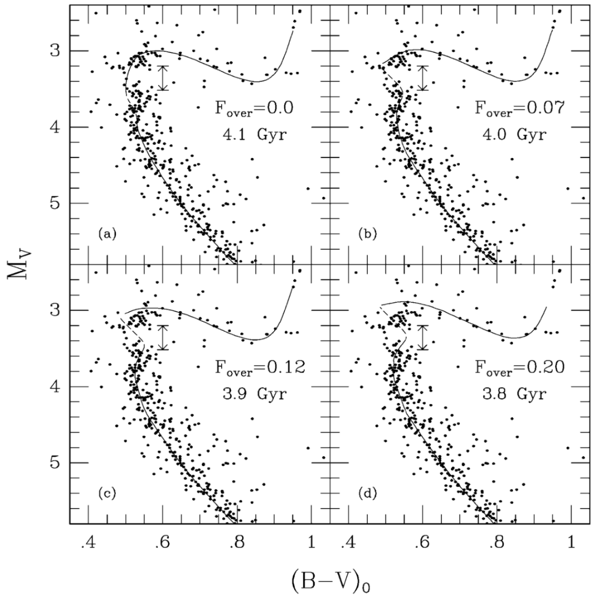

Figure 5. Theortical isochrones fitted with varying values of age and overshooting, $F_{\rm over}$ as shown by Vandenberg (1985)

changes of the estimated parameters in table 1. Two developmental methods have been outlined by Naylor & Jeffries (2006) and Valle et al. (2021), but there is no generally agreed-upon methodology when measuring the 'goodness' of fit. A chi-squared (χ^2) test can be performed using `scipy` and easily implemented. The following expression can be used to perform the test,

$$\chi_c^2 = \sum \frac{(O_i - E_i)^2}{E_i} \tag{14}$$

Where O is the observed value, and E is the expected value. After each interpolation, the isochrone can be compared against the cluster data for each ith point taking E_i to be the closest point on the isochrone. This will be taken as the $(O-E)^2/E$ component to be summed. The code suite created by Naylor & Jeffries (2006) runs quickly and provides similar results as produced in fig. 4 with much more rigour on how well the isochrone fits. However, interpolation of $F_{\rm over}$ parameters does not appear to be implemented as of the most recent stable release.

8. OPEN CLUSTERS HOME IN THE GALAXY

Finally, following the calibration of both magnitude and the theoretical isochrone, an estimation of age, distance, and spatial distribution can be made. Distance and age at this point will be calculated. Along with this any imposters in the stellar population will be removed if spotted as outliers during magnitude or metallicity calibration. From here, the cluster can be classified, and comments can be made on the stellar evolution of the cluster and evolution in both the galactic bulge and arms or any of the previously discussed parameters (Friel 1995).

REFERENCES

Bradley, L., Sipőcz, B., Robitaille, T., et al. 2020, astropy/photutils: 1.0.0, 1.0.0, Zenodo, doi: 10.5281/zenodo.4044744

Budding, E., & Demircan, O. 2007, Introduction to astronomical photometry (Cambridge University Press)

Choi, J., Dotter, A., Conroy, C., et al. 2016, ApJ, 823, 102, doi: 10.3847/0004-637X/823/2/102

Friel, E. D. 1995, Annual Review of Astronomy and Astrophysics, 33, 381, doi: 10.1146/annurev.aa.33.090195.002121

Howell, S. B. 2006, Handbook of CCD Astronomy, 2nd edn., Cambridge Observing Handbooks for Research Astronomers (Cambridge University Press), doi: 10.1017/CBO9780511807909

Karaali, S., Bilir, S., Ak, S., Yaz, E., & Coşkunoğlu, B. 2011, Publications of the Astronomical Society of Australia, 28, 95–106, doi: 10.1071/AS10026

Nataf, D. M., Gould, A., Fouqué, P., et al. 2013, ApJ, 769, 88, doi: 10.1088/0004-637X/769/2/88

Naylor, T., & Jeffries, R. D. 2006, MNRAS, 373, 1251, doi: 10.1111/j.1365-2966.2006.11099.x

Paxton, B., Schwab, J., Bauer, E. B., et al. 2018, ApJS, 234, 34, doi: 10.3847/1538-4365/aaa5a8

Stetson, P. B. 1987, PASP, 99, 191, doi: 10.1086/131977

Tojeiro, R., Wilkins, S., Heavens, A. F., Panter, B., & Jimenez, R. 2009, The Astrophysical Journal Supplement Series, 185, 1–19, doi: 10.1088/0067-0049/185/1/1

Valle, G., Dell'Omodarme, M., & Tognelli, E. 2021, A&A, 649, A127, doi: 10.1051/0004-6361/202140413

Vandenberg, D. A. 1985, ApJS, 58, 711, doi: 10.1086/191055

VandenBerg, D. A., & Stetson, P. B. 2004, PASP, 116, 997, doi: 10.1086/426340

Pathfinding with the Old Breed: Using the Old Open Clusters for Galactic Tracing

PI: O. Johnson

1. Abstract

The study of open clusters has been a keystone in the study of the Milky Way. They are large scale stellar laboratories and lend themselves to the study of stellar evolution due to the homogeneity of their stellar population. The use of open clusters in mapping the milky way is an old process of comparing the age of open clusters against their spatial distribution. With the progression of photometry and high-resolution astrometric studies, many open clusters can be re-examined with more detail on both the cluster parameter and the interplay between cluster age and distribution throughout the galactic disk. 8 clusters of varying age and disk location are proposed for a total of 58 minutes.

2. Description of the proposed programme

A) Scientific Rationale:

Open clusters give one of the most relevant insights into both stellar and galactic evolution. Open clusters are classified as populations of sparsely bound stars. The study of open clusters is done primarily by studying stellar populations by creating a colour-magnitude diagram (CMD). CMDs allow for the estimation of age, distance, metallicity, among other attributes of an open cluster. This is specifically done by the fitting of stellar isochrones, which are fitted to the CMD of the open cluster. Stellar isochrones are ways of fitting data on a CMD that allow the stellar evolutionary path to being determined directly from optical photometry, see Montgomery et al. (1990) for a comprehensive example.

This has been shown to give accurate insight into both stellar and galactic evolution.

It has been shown by van den Bergh & McClure (1980) that open clusters with an age of 1 Gyr are preferentially located on towards the galactic anti-centre. Oort (1950) found that there was an underabundance of old clusters relative to the number extrapolated by the population of their younger counterparts assuming uniform stellar formation rate throughout the galactic disk during its lifetime. Spitzer (1958) deemed that the small number of old clusters was from disruptive interactions massive clouds towards the galactic core. However, the first large scale study of open clusters analysed by Janes et al. (1988) found that the disruptive processes were too efficient to support the population of the old breed of open clusters. Moreover, this first large scale analysis of the Lynga catalogue (Lynga, 1982) found that the resultant cluster populations were determined through a nuanced relationship between inherent cluster properties, internal dynamics and overall environment in the galaxy.

Since then, Gaia has performed a large astrometric and photometric survey giving the first panoptic view of the galactic disk, which has allowed for a growth in catalogues like WEBDA. Studies such as Cantat-Gaudin et al. (2020) have classified reddening, distance and age of ~ 2000 clusters. Thus since many galactic tracing surveys have been completed, there has been a substantial improvement on the means to determine cluster parameters through isochrone fitting using supplementary high-resolution spectroscopic surveys such as Tojeiro et al. (2009) and Jackson et al. (2022).

Despite recent surveys, there are still many open clusters that lack sufficient cataloguing and parameters. This study proposes to study the position of open clusters in Milkey Way's disk and show how the inclusion of modern isochrone fitting can consolidate previous research in galactic tracing such as Lynga (1982).

B) Immediate Objective:

The observation expedition proposes to observe a sample of open clusters from the WEBDA catalogue of varying ages and disk positions. This follows on from studies such as Lynga (1982) and VandenBerg & Stetson (2004). However, with the added advantage of using stellar isochrones from the MIST catalogue. These isochrones take full advantage of recent astrometric studies and improved isochrone models (see. Choi et al., 2016). This allows parameters such as reddening, metalicity and convection overshooting to be estimated to a more satisfactory degree than prior studies of a similar nature. This includes things such as

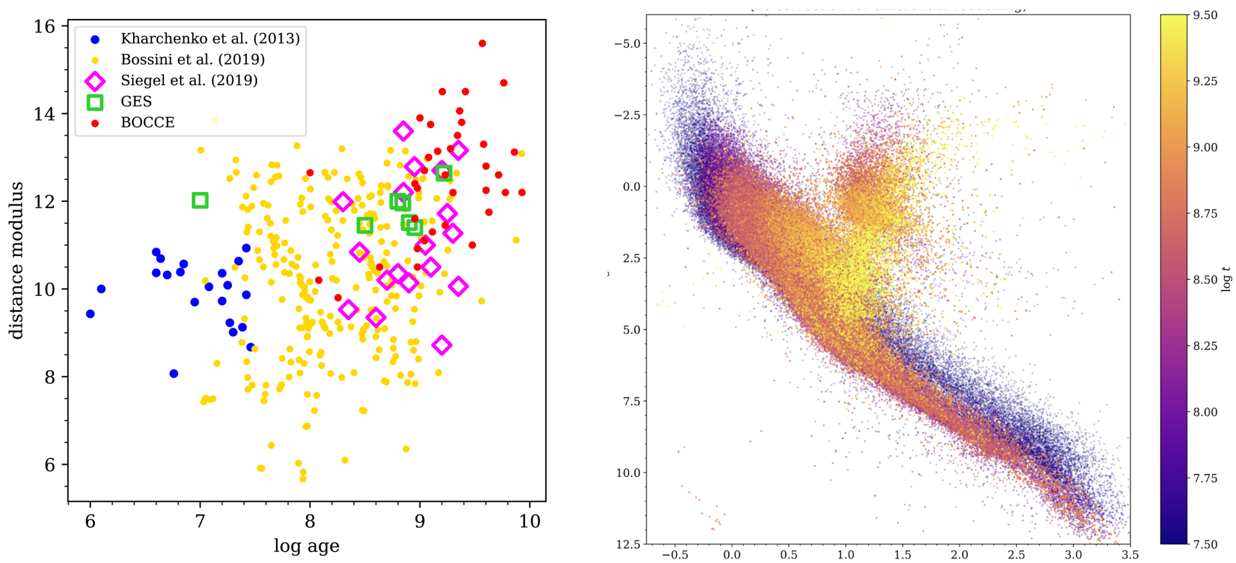

(a) Distance modulus against the log age of a sample of open-clusters.

(b) A comprehensive Hertzprung-Russell diagram which is colour-coded by cluster age.

Figure 1: Both plots provided by Galactic tracing study by Cantat-Gaudin et al. (2020).

the oversight of convection overshooting when fitting isochrones as shown by VandenBerg & Stetson (2004). Convection overshooting shows large discrepancies in the later stage of the main sequence. Correcting for this allows for cluster age to be interpolated at finer increments as a more reliable fit can be attained.

Each cluster's stellar population will be analysed and classified based on the Trumpler system (Trumpler, 1930). This will be done by means of photometric analysis using `photoutils` to create CMD plots for each cluster (fig. 1 (b)). Following classification, a plot against distance age (fig. 1 (a)) The distance of the cluster will be plotted against age to examine the abundance of older clusters on the outer disk and comment on the disruptive interactions with molecular clouds. Using provided CMD's, the presence of pre-main-sequence stars towards the galactic centre will examine. The main-sequence stage of intermediate aged clusters will also be examined. Following this, a comment on the interplay between age, distance and galactic environment can be postulated. Giving insight both into the shape of the milky way disk through tracing distance progression of clusters at varying ages.

3. Justification of requested observing time, feasibility and visibility

This observation expedition proposes the observation of 12 open clusters of varying age. The clusters will be broken into three sets. Each set will comprise of 3 clusters of the following age categories, 'Young': age $<$ 200 Myr, 'Intermediate': 200 Myr $<$ age $<$ 1 Gyr and 'Old': 1 Gyr $<$ age. Each set will be observed at different areas of the galactic disk, see fig. 3.

A list of suitable targets with backup targets can be found in table 1. Table 1 is organised by right ascension (RA) into groups (segregated) with varying ages in each RA window. A list of backup targets is also listed to be compatible with the corresponding group for the primary, and the study suggested if the main objective is not feasible.

Exposure time was selected to have a signal to noise ratio (SN) of $\sim$10 for the most feint members of a cluster population. However, doing this in some cases will cause either source to be saturated if bright or too noisy if feint. In this case, the exposure that adequately observed $\sim$98% of the stellar population was chosen (fig. 2).

Each target will be observed in both **B** and **V** Johnson filters. As mentioned, each cluster will have SN

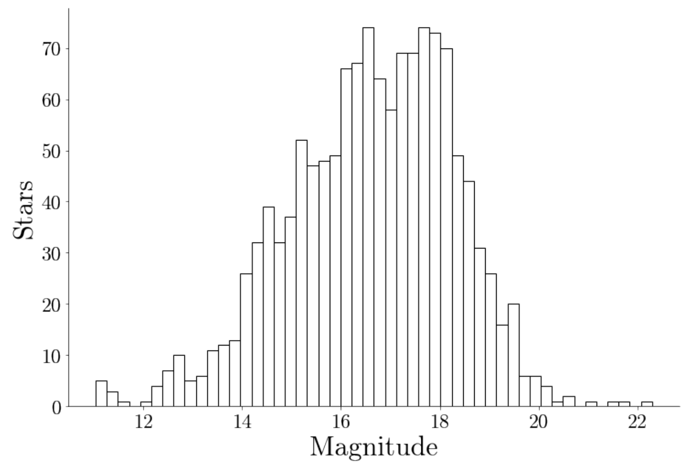

Figure 2: Example distribution of magnitude for stellar population of NGC2129

$\simeq$10 for most feint members of the population. In turn, this provides an instrumental error on the magnitude of 0.1 or less. If inadequate samples from across the galactic disk are attained for a sufficient number of clusters, further numbers can be taken from archived data. In the case where the primary objective *cannot* be completed, the observed data can be homogenised and used to catalogue membership and classification of each cluster, producing membership probability along with Trumpler classification of each cluster. This would provide cataloguing of poorly documented clusters see table 1. As discussed with the use of MIST isochrones, ages, convections, and metalicities would be investigated to produce an elegant stellar catalogue for all observed clusters. This secondary objective would take a similar form to VandenBerg & Stetson (2004).

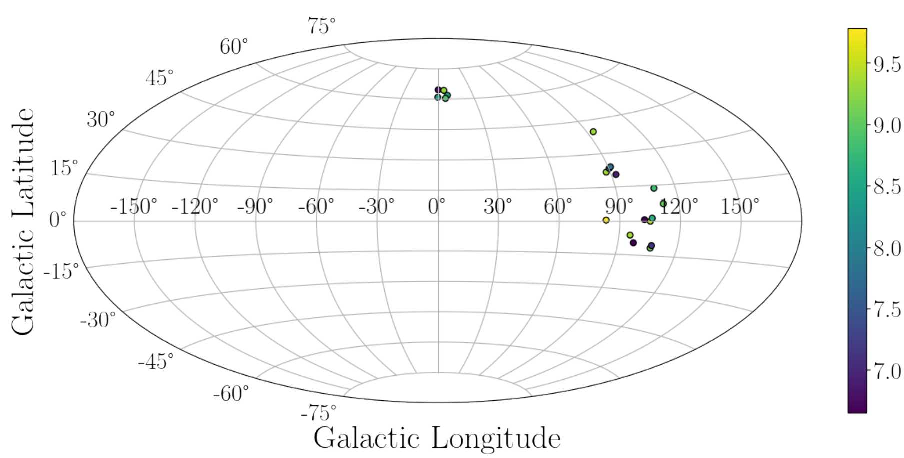

Figure 3: Suggested open-cluster targets plotted in Galactic co-ordinates. Where the cluster age is shown using the color bar. Targets taken from the WEBDA database.

4. Previous/complementary data

A) Preliminary Data:

Lynga (1982)[1] provided the first large scale database on open cluster it has all discussed parameters with specific bib information on where to find any missing parameters. WEBDA[2] is an online version of the BDA created by Mermilliod (1995) it was the primary means of sourcing targets of it has collected most published data on open clusters with over 700 entries from the BDA and cross-references with other available catalogues. WEBDA provided all data seen in table 1. SIMBAD[3] was also used to cross-reference WEBDA during target selection process.

B) Complementary Data:

As there is no spectroscopic photometry performed or use of a U filter, the colour excess and the metalicity will need to be referenced. In the case of metalicity, the values will be inferred directly from observations through isochrones but will need to be supplemented by spectroscopic databases such as Tojeiro et al. (2009). The second Gaia data release can be used for supporting astrometric data provided by studies such as Cantat-Gaudin et al. (2020). In the case where a larger sample size of clusters can give extra data, Jackson et al. (2022) and Bonatto et al. (2006).

References

Bonatto, C., Kerber, L. O., Bica, E., & Santiago, B. X. 2006, Astronomy and Astrophysics, 446, 121

Cantat-Gaudin, T., Anders, F., Castro-Ginard, A., et al. 2020, Astronomy and Astrophysics, 640, A1

Choi, J., Dotter, A., Conroy, C., et al. 2016, Astrophysical Journal, 823, 102

Jackson, R. J., Jeffries, R. D., Wright, N. J., et al. 2022, Monthly Notices of the RAS, 509, 1664

Janes, K. A., Tilley, C., & Lynga, G. 1988, Astronomical Journal, 95, 771

Lynga, G. 1982, Astronomy and Astrophysics, 109, 213

Mermilliod, J.-C. 1995, in Information & On-Line Data in Astronomy, ed. D. Egret & M. A. Albrecht, Vol. 203, 127

Montgomery, K., Marschall, L., & Janes, K. A. 1990, in Bulletin of the American Astronomical Society, Vol. 22, 1288

Oort, J. H. 1950, Bulletin Astronomical Institute of the Netherlands, 11, 91

Spitzer, Lyman, J. 1958, Astrophysical Journal, 127, 17

Tojeiro, R., Wilkins, S., Heavens, A. F., Panter, B., & Jimenez, R. 2009, The Astrophysical Journal Supplement Series, 185, 1–19, doi: 10.1088/0067-0049/185/1/1

Trumpler, R. J. 1930, Lick Observatory Bulletin, 420, 154, doi: 10.5479/ADS/bib/1930LicOB.14.154T

van den Bergh, S., & McClure, R. D. 1980, Astronomy and Astrophysics, 88, 360

VandenBerg, D. A., & Stetson, P. B. 2004, Publications of the ASP, 116, 997

[1] https://heasarc.gsfc.nasa.gov/W3Browse/star-catalog/lyngaclust.html

[2] https://webda.physics.muni.cz/

[3] http://simbad.u-strasbg.fr/simbad/

Cluster Name	**RA**	**DEC**	**Age**	**Modlus**	**Diameter**	**B exp.**	**V exp.**	**Total Exp.**	**Obs. Window**
	HH:MM:SS	DEG:HH:SS	log	$m - M$	arcmin	seconds:frames	seconds:frames	seconds	(date) time
King 15	00 32 54	61 52 00	8.40	14.67	3	60 : 4	60 : 4	480	(a)21:00 - 05:00
Stock 18	00 01 37	64 37 3	6.78	14.41	6	60 : 3	60 : 3	360	(a)21:00 - 05:00
King 1	00 22 04	64 22 5	9.3	13.56	9	60 : 3	45 : 4	360	(a)21:00 - 05:00
Berkeley 20	05 33 00	00 13 00	9.78	14.99	2	45 : 2	30 : 3	180	(9)21:00 - 01;30
NGC 2192	06 15 17	39 51 18	9.30	12.11	5	60 : 4	60 : 2	240	(12) 22:30 - 05:30
vdBergh 80	06 30 48	-09 40 00	6.65	0.38	2	110: 2	65 : 3	415	(11) 22:00 - 02:00
Bochum 2	06 48 54	00 23 00	6.665	0.831	1	110: 2	65 : 3	415	(10) 22:00 - 02:00
Berkeley 34	07 00 24	-00 15 00	9.45	15.8	2	60 : 4	120: 3	600	(10) 22:00 - 03:00
NGC 2355	07 16 59	13 45 00	8.85	12.08	7	60 : 4	45 : 4	420	(9) 21:00 - 04:00
Backup targets									
Berkeley 2	00 25 18	60 24 00	8.90	16.08	2	60 : 4	115: 2	410	(a) 21:00 - 05:00
Berkeley 21	05 51 42	21 47 00	9.34	15.85	5	60 : 3	115: 2	350	(13) 21:00-03:00
NGC 2129	06 00 41	23 19 06	7.318	12.9	5	60 : 4	60 : 4	480	(11) 22:30–04:00
Berkeley 73	06 22 00	-06 21 00	9.36	14.5	2	100: 4	100: 4	800	(9)21:00 - 02;00
Berkeley 76	07 06 41	-11 43 30	9.18	17.21	5	100: 4	100: 4	800	(11) 22:30–03:30
Haffner 3	07 04 00	-06 08 00	/	/	/	100: 4	120: 3	760	(12) 22:00–02:30
NGC 2394	07 28 36	07 05 12	9.05	9.25	8	60 : 4	120: 3	600	(9) 21:00-03:30

Table 1: Propesed Open Clusters for obsercation using WEBDA catalog. For the observation window most targets are obserble each night however preffered observation times have been listed. (a) denotes that there is no favoured night for observation.